CERTIFICATION OF APPROVAL

Study of Liquid Flow with Bubbles in Pipes

by

Pau Shang Pei

A project dissertation submitted to the
Mechanical Engineering Programme
Universiti Teknologi PETRONAS
in partial fulfilment of the requirement for the
BACHELOR OF ENGINEERING (Hons)
(MECHANICAL ENGINEERING)

Approved by,

_____

(Ir. Dr. Shaharin Anwar Sulaiman)

UNIVERSITI TEKNOLOGI PETRONAS

TRONOH, PERAK

January 2010

CERTIFICATION OF ORIGINALITY

This is to certify that I am responsible for the work submitted in this project, that the original work is my own except as specified in the references and acknowledgements, and that the original work contained herein have not been undertaken or done by unspecified sources or persons.

_____

PAU SHANG PEI

ABSTRACT

In oil and gas industry, fluid flow in pipe is a common occurrence and creates several critical issues. Produced wellhead fluids are often mixtures of different compounds of carbon, all with different densities, vapor pressures, and other characteristics. The change of pressure and temperature results in the evolving of gas as the production is lifted up to higher elevation. This multiphase flow complicates the flow metering. Cavitation, which involves the evolving and collapsing of bubbles in liquid, is another problem related to fluid flow. The existence of bubbles in liquid flow causes unfavorable issues for example pressure drop through pipeline, vibration, cavitation and multiphase metering. Thus, the objective of this project is to study the behavior of bubbles in flowing liquid and understand how it affects the fluid flow. Literature reviews on similar experimental works, equipments and devices and simulations are reviewed for better understanding and to

improve current ideas on this project. A lot of the experiments conducted previously involve fluid flow in pipes, flowing either downward or upward. The methodology, which keeps track of the project work, shows the project is completed on time. Experiment setup shows how the two mechanical equipments, cavitation pump and Laser Doppler Anemometry/Phase Doppler Anemometry (LDA/PDA), are adjusted and reoriented to better tolerate with the mechanical constraints. The project proceeds with data analysis, at which the sauter mean diameter is calculated and graphs are plotted along with an illustration of bubbles. Velocity profiles are constructed to shows the trend of the characteristics of bubbles at different points along the pipe line. From the results, it is clear that the factors affecting the behavior of bubbles are water flow rate, boundary layer, buoyancy force, drag and friction.

ACKNOWLEDGEMENTS

I would like to acknowledge the following people for their assistance and support throughout the process of project completion.

Firstly, I would like to thank Universiti Teknologi PETRONAS for providing me with such a great opportunity to perform in final year project. This project, which is completed within two semesters' time, has obviously sharpened my engineering knowledge and skills, i.e. communication skill, analytical thinking, ability to work independently and team work.

Next, I would like to thank Ir. Dr. Shaharin Anwar Sulaiman, who willingly accepts me as a student undertaking final year project under his supervision. I truly appreciate and respect the way he contributes his effort and time to guide me all the time to improve on the project. Not only he has shared with me the fundamental engineering knowledge, but he has also made me realize that final year project is actually a stepping stone to prepare me for working life in the future. His critics and praises would always be words of encouragement for me.

I would like to thank Mr. Zailan Alang Ahmad. He has guided me in all issues and consequences related to mechanical equipments and operations. He never hesitates to give assistance when the experiments are conducted.

Besides, I would like to acknowledge Mr. Khairul Anwar, who gives me helping hand in performing risky experiments. I truly appreciate the time and energy he has given by assisting in setting up and conducting the experiments.

I would like to express my gratitude to all my friends who have contributed to my project, especially those who willingly help out as my man power. Without them, I would say the process of the project would not be as smooth.

I believe, without anyone of them, I would never have come this far and complete my final year project with such success. Thank you!

TABLE OF CONTENTS

CERTIFICATION OF ORIGINALITY ii

ABSTRACT ii

ACKNOWLEDGEMENTS iii

TABLE OF CONTENTS iv

LIST OF FIGURES vii

LIST OF TABLES ix

ABBREVIATIONS ix

NOMENCLATURES ix

CHAPTER 1: INTRODUCTION 1

1.1 Background of Study 1

1.1.1 Fluids and Fluid Flow 1

1.1.2 Cavitation 1

1.1.3 Produced Wellhead Fluids 2

1.1.4 Crude Oil 3

1.1.5 Multiphase Flow 3

1.1.6 Gas-lift 4
1.2 Problem Statement 4
1.3 Objectives and Scope of Study 5
1.3.1 Objectives 5
1.3.2 Scope of Study 5
CHAPTER 2: LITERATURE REVIEW AND THEORY 5
2.1 Experimental Studies 6
2.1.1 Bubble Size in Turbulent Air-water Flow through Horizontal Pipes 6
2.1.2 Bubble and Liquid Turbulence Characteristics of Bubbly Flow 6
2.1.3 Effect of Bubble Size in Turbulent Bubbly Downflow in a Vertical Channel 7
2.1.4 Bubbling Generation Technology and Application Using City Water Pressure 7
2.1.5 Visualization of the Flow around a Bubble Moving in a Low Viscosity Liquid 8
2.2 Theories 9
2.2.1 Disperse Flows 9
2.2.2 Natural or Forced Fluid Flow 9
2.2.3 The Control of Fluid Flow 10
2.2.4 Pressure Difference between Two Phases 10
2.2.5 The Development of Velocity Boundary Layer 11
2.2.6 Sauter Mean Diameter 12
2.3 Equipment and Devices 14
2.3.1 Optical Investigation 14
2.3.2 Experiments on the Effect of Acceleration on the Drag of Tap Water Bubbles 14
2.3.3 Velocity Measurements of Liquid and Gaseous Phase of Bubbles Rising in Water 15
2.4 Numerical Simulations 16
CHAPTER 3: METHODOLOGY 17
3.1 Gantt Chart and Milestones 18
3.2 Project Process Flow 20
CHAPTER 4: EXPERIMENT SETUP 22
4.1 Cavitation Pump Rig 22
4.1.1 Water Pump 24
4.1.2 Air Pump 25
4.1.3 Pipe System 26
4.1.4 Modification of Pipe 28

4.2 Laser Doppler Anemometry/Phase Doppler Anemometry 30
4.2.1 Laser Doppler Anemometry 30
4.2.2 Phase Doppler Anemometry 33
4.2.3 Integrated PDA Solutions 34
4.2.4 LDA/PDA Orientation in UTP Lab 35
4.3 Vane Anemometer 36
4.4 Experiment Setup 37
4.4.1 Laser Beam Intersection 37
4.4.2 Experiment Trial using Water Spray 38
4.4.3 Combination of LDA/PDA and Cavitation Pump 38
4.4.4 Bubble Injection and Laser Beam Intersection Point 39
4.4.5 Data Acquisition 39
4.4.6 BSA Flow Software Data Sheet 40
CHAPTER 5: RESULTS AND DISCUSSION 41
5.1 Five gpm Water Flow Rate 43
5.1.1 Velocity Profile 43
5.1.1 Sauter Mean Diameter Analysis 45
5.2 Ten gpm Water Flow Rate 48
5.2.1 Velocity Profile 48
5.2.1 Sauter Mean Diameter Analysis 50
5.4 Fifteen gpm Water Flow Rate 53
5.4.2 Velocity Profile 53
5.4.1 Sauter Mean Diameter Analysis 55
5.5 Twenty gpm Water Flow Rate 58
5.5.2 Velocity Profile 58
5.5.1 Sauter Mean Diameter Analysis 60
5.6 Bubbles Image 62
5.7 Effect of Boundary Layer on Distribution of Bubbles 64
CHAPTER 6: CONCLUSION AND RECOMMENDATION 64
5.1 Conclusions 64
5.2 Recommendations 66
REFERENCES 67
APPENDICES 70

LIST OF FIGURES

Figure 1.1: Gas-lift system 4
Figure 2.1: Measuring by high-speed camera 8
Figure 2.2: Different diameter ranges of bubbles generated by co-developed nozzle 8
Figure 2.3: Schematic of experimental setup 9
Figure 2.4: The development of the velocity boundary layer in a pipe for laminar flow 11
Figure 2.5: Schematic of variable chamber bubble injector 15
Figure 2.6: Bubble swarm generator 16
Figure 2.7: The FLUENT fuel pump geometry 17
Figure 3.1: Process flow diagram of the project 21
Figure 4.1: Cavitation pump rig 22
Figure 4.2: Schematic diagram of cavitation pump to be used with LDA/PDA 23
Figure 4.3: Water circulation in cavitation pump rig 23
Figure 4.4: Water pump 24
Figure 4.5: DC motor speed control 24
Figure 4.6: Air pump 25
Figure 4.7: The introduction of bubbles using air pump 25
Figure 4.8: Air flow valve 26
Figure 4.9: Pipe elbow 26
Figure 4.10: Position of the specific pipe part for data collection 26
Figure 4.11: Pipe length Figure 4.12: Pipe inner and outer diameter 27
Figure 4.13: Water flow meter 27
Figure 4.14: Control valve 28
Figure 4.15: Bubble injection point at modified pipe part 28
Figure 4.16: The replacement of modified pipe part and cavitation pump system orientation 29

Figure 4.17: Modified cavitation pump rig due to the constraints of LDA/PDA 29
Figure 4.18: Laser Doppler Anemometry (Dantec Dynamics, 2010) 30
Figure 4.19: The probe and the probe volume 31
Figure 4.20: Doppler frequency to velocity transfer function for a frequency shifted LDA system 32
Figure 4.21: Beams added to the optics in a plane perpendicular to the first beams to measure two velocity components 33
Figure 4.22: Phase Doppler Anemometry 33
Figure 4.23: Light scattering, Φ versus particle size, D 34
Figure 4.24: LDA/PDA orientation in UTP lab 35
Figure 4.25: Laser source for LDA/PDA 36
Figure 4.26: Transmitting and receiving probes 36
Figure 4.27: Vane anemometer set 37
Figure 4.28: Laser beam intersection 37
Figure 4.29 Experiment trial using water spray 38
Figure 4.30 Experiment trial using water spray 38
Figure 4.31: Combination of cavitation pump and LDA/PDA 39
Figure 4.32: Laser beams intersect inside pipe with bubble injection at the inlet 39
Figure 4.33: The positions of the points for data collection 40
Figure 4.34: Coordination of data points 40
Figure 4.35: BSA Flow Software data sheet example 41
Figure 5.1: Horizontal velocity profile (5 gpm) 43
Figure 5.2: Vertical velocity profile (5 gpm) 43
Figure 5.3: Bubble diameter illustration (5 gpm) 46
Figure 5.4: D_{32} versus horizontal displacement from center of pipe 47
Figure 5.5: Horizontal velocity profile (10 gpm) 48
Figure 5.6: Vertical velocity profile (10 gpm) 48
Figure 5.7: Bubble diameter illustration (10 gpm) 51
Figure 5.8: D_{32} versus horizontal displacement from center of pipe 52
Figure 5.9: Horizontal velocity profile (15 gpm) 53
Figure 5.10: Vertical velocity profile (15 gpm) 53
Figure 5.11: Bubble diameter illustration (15 gpm) 56
Figure 5.12: D_{32} versus horizontal displacement from center of pipe 57
Figure 5.13: Horizontal velocity profile (20 gpm) 58
Figure 5.14: Vertical velocity profile (20 gpm) 58

Figure 5.15: Bubble diameter illustration (20 gpm) 60
Figure 5.16: D_{32} versus horizontal displacement from center of pipe..... 61
Figure 5.17: Picture of bubbles at different water flow rates..... 63
Figure 5.18: Effect of boundary layer on distribution of bubbles……...64
Figure 6.1: Horizontal velocity prediction..... 67
Figure 6.2: Vertical velocity prediction..... 67

LIST OF TABLES

Table 3.1 Gantt chart and milestone for FYP I.....19

Table 3.2 Gantt chart and milestone for FYP II.....20

Table 5.1: Unit conversion for motor speed and water flow rate.....43

ABBREVIATIONS

LDA	Laser Doppler anemometry
PDA	Phase Doppler anemometry
PVC	Polyvinyl chloride

NOMENCLATURES

d_f	Fringe distance (m)
D	Particle size (μm)
D_{10}	Mean arithmetic diameter (μm)
D_{20}	Surface mean diameter (μm)
D_{30}	Volume mean diameter (μm)
D_{32}	Sauter mean diameter (μm)
D_{43}	Volume moment mean diameter (μm)

f_D	Doppler frequency (Hz)
F	Phase difference between signals from two detectors
I	Current (A)
k	Number of ranges
L_e	Entrance length (m)
n_i	Number of droplets
r	Sphere radius (μm)
t	Time (s)
U	Particle velocity (m/s)
V	Volts
V	Velocity (m/s)

GREEK SYMBOLS

λ	Wavelength of laser light (m)
Φ	Light scattering (°)
θ	Angle between beams (°)

CHAPTER 1

INTRODUCTION

Chapter 1 presents the project as a whole and identifies the current issues related to it. Identification of the problems leads to the establishment of problem statement which contributes to the objectives of the study.

Background of Study

1.1.1 Fluids and Fluid Flow

In an oil and gas plant, there are broad applications of pipes. Pipes come in different sizes, materials, inner and outer diameter, wall thickness, length and capacities. In this project, fluids in pipes are examined. A fluid defined as a substance in the liquid or gas phase (Cengel and Cimbala, 2006). Both liquid and gas phases are considered in this project. Examples of liquid are water, oil and gasoline while examples of gas would be atmospheric air, evaporated oil, methane and others. Flows in which the fluid viscosity is important can be of two types: laminar and turbulent (Kundu and Cohen, 2008). Laminar flow is described as a well ordered pattern whereby fluid layers are assumed to slide over one another (Shames, 2003). Then, a transition is taking place from the previous well-ordered flow, which may be considered as laminar flow, to an unstable type of flow. This flow is called the transitional flow. As the flow rate was increased beyond a critical value, the flow broke into an irregular motion, indicating the presence of macroscopic mixing motion perpendicular to the direction of flow and such chaotic motion is called turbulent flow (Kundu and Cohen, 2008). Turbulent flow is the most common type of flow. Laminar flow does occur in situations with fluids of greater viscosity-e.g. in bearing with oil as lubricant (Sleigh, 2009).

1.1.2 Cavitation

Some liquids in pipes would generate low pressure and cause the liquid vaporize, which is to boil at room temperature. This is when the local absolute pressure of the liquid falls below its vapor pressure (Andrews, 2004). The vaporized liquid forms bubbles that are carried by the flow to the downstream locations. The bubbles will collapse rapidly and violently when the local absolute pressure increases due to kinetic forces being imparted

by the impeller. These collapsing bubbles can generate localized high pressure fluctuations (Liu, 2003). Cavitation is the rapid formation and collapse of these vapor bubbles (Andrews, 2004). Any solid that comes into contact with the bursting bubbles can become severely damaged in a relatively short time. The damage is usually in the form of pitting or cavities and it is called cavitation (Liu, 2003). When cavitation occurs in centrifugal or impeller pump, it usually damages the running blades and parts of the pump casing. Pumps damaged by cavitation not only lose efficiency but also may develop vibration and other problems (Liu, 2003). Cavitation is not limited by heat transfer but only inertial effects in the surrounding liquid. Cavitation is therefore an explosive (and implosive) process that is far more violent and damaging than the corresponding bubble dynamics of boiling (Brennen, 2005). One of the examples of cavitation would be a nickel alloy pump impeller blade exposed to a hydrochloric acid medium.

1.1.3 Produced Wellhead Fluids

Produced wellhead fluids are complex mixtures of different compounds of hydrogen and carbon, all with different densities, vapor pressures, and other physical characteristics (Stewart, 2008). The pressure in a black oil reservoir at discovery will be either higher than the bubble-point pressure of the oil or equal to the bubble-point pressure (McCain, 1990). This initial reservoir pressure will not be below the bubble-point pressure of the reservoir oil. Production into the wellbore will consist solely of liquid. As a well stream flows from the hot, high-pressure petroleum reservoir, it experiences pressure and temperature reductions (Stewart, 2008). Gases evolve from the liquids and the well stream changes in character. The velocity of the gas carries liquid droplets, and the liquid carries gas bubbles (Stewart, 2008). At first this free gas does not move. However, as pressure continues to decrease, the volume of gas in the pore space increases and the gas begins to move to the wellbore (McCain, 1990). Low viscosity and other factors cause gas to flow through the reservoir more readily than oil.

1.1.4 Crude Oil

Crude oil is another issue that deals with bubbles. Crude oil appears in three phases in reservoirs: gas, liquid and solid. Metering of multiphase production from oil and gas wells is required for well control, reservoir management, custody transfer, fiscal obligations and leak detection in flow lines (Manning and Thompson, 1995). Multiphase metering defined to be the measurement of the individual flow rates of natural gas, crude oil, and water when all three phases are flowing simultaneously in a pipe. Multiphase flow metering is inherently much more difficult than single-phase flow measurement. Single-phase flows exhibit only three regimes: laminar, transition, or turbulent; these regimes occur over easily defined Reynolds number ranges (Manning and Thompson, 1995). In marked contrast, numerous regimes, such as annular, bubbly, chum, slug, stratified, wavy, are observed in multiphase flow (Manning and Thompson, 1995). Occurrence of these regimes depends on many parameters such as pipe geometry, line orientation (vertical, inclined and horizontal), flow direction (up and down) as well as fluid properties and flow rates.

1.1.5 Multiphase Flow

There are two kinds of multiphase flow: dispersed flows and separated flows. By disperse flow we mean those consisting of finite particles, drops or bubbles (the dispersed phase) distributed in a connected volume of the continuous phase (Brennen, 2005). Thus, for this particular project, only disperse flow is to be considered and studied. For frictional loss in a disperse flow, vertically-oriented pipe flow can experience partially separated flows in which large relative velocities develop due to buoyancy and the difference in the densities of the two-phases or components (Bennen, 2005). These large relative velocities complicate the problem of evaluating the pressure gradient.

According to Longo (2006), many natural and technical fluid flows are two-phase flows because of the entrapment or release of air. In high-speed flows in open channels, air is entrapped by macroturbulence reaching the free surface. Examples of air entrapment are at the toe of a hydraulic jump and in most breaking waves. Vapour bubbles develop as a result of cavitation.

1.1.6 Gas-lift

Another field of interest would be gas-lift. Generally, it is which gas bubbles are injected from the bottom of a pipe where a liquid is flowing so as to reduce the gravitational pressure drop (Descamps et al., 2008). According to Schlumberger (2009), in oilfield, gas lift is referred to as an artificial-lift method in which gas is injected into the production tubing in order to reduce the hydrostatic pressure of the fluid column. This allows the reservoir liquids to enter the wellbore at a higher flow rate as a result of reduction in bottomhole pressure. With this, the density of the fluid (oil or water) will be reduced. The injection gas, continuously or intermittently, is typically conveyed down the tubing-casing annulus and then enters the production train through a series of gas-lift valves. The amount of gas injected varies with well conditions and geometries. Too much or too little injected gas will result in less than maximum production. Thus, a gas-lift system is very important in order to provide production energy by injecting gas into the production fluid column to reduce hydrostatic pressure. This will then improve reservoir production.

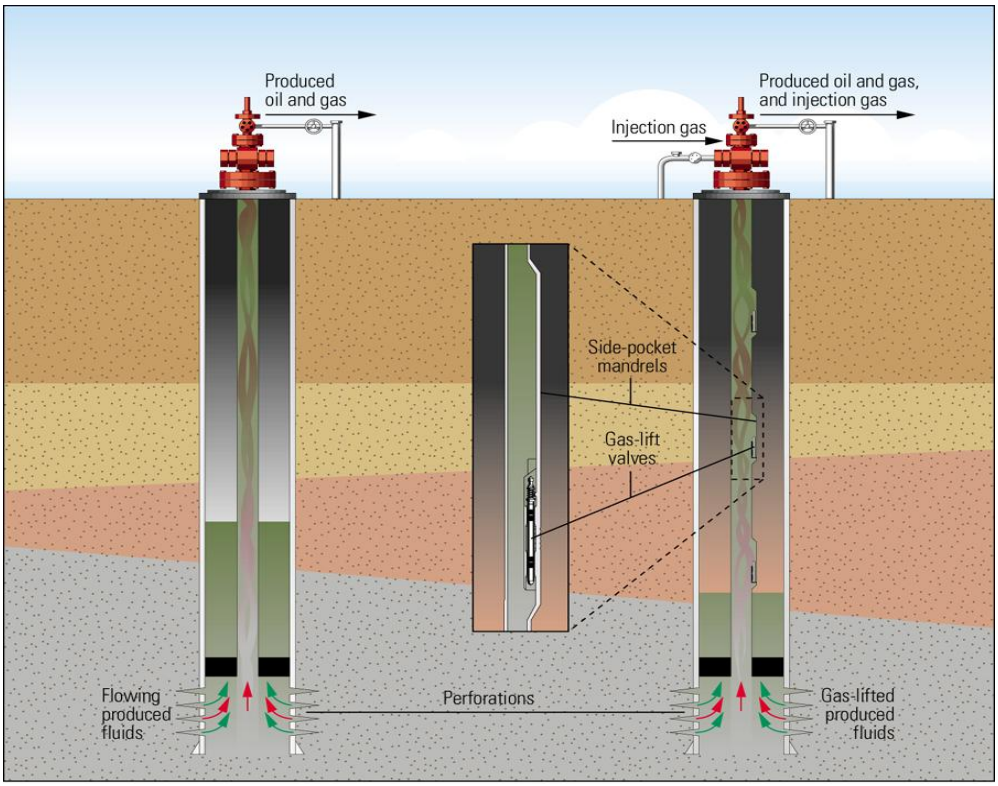

Figure 1.1: Gas-lift system (Schlumberger, 2009)

Problem Statement

The existence of bubbles in liquid flow causes problems in various applications involving pipelines. These problems include pressure drop through pipeline, vibration, cavitation and multiphase metering. Bubble sizes are critical in determining the production rate of gas lift mechanism. The control of bubbles would help to reduce pressure drop and vibration as it could minimize energy loss, besides reduces the chances of cavitation. Multiphase metering could be less complicated as the number of phases is decreased when bubbles are removed. However, the characteristics of bubbles in flowing liquid are complicated, partly due to the effect of drag, viscosity of the fluids involved, friction and wall shearing stress. Thus, a fundamental study of the behavior of bubbles in liquid flow in pipe is required.

Objectives and Scope of Study

1.3.1 Objectives

The objective of the present project is to study the behavior of bubbles in flowing liquid in pipes. The information from this work would enable investigation of the effects of the bubbles in various pipeline applications.

1.3.2 Scope of Study

The scope of study would cover experimental study of the characteristics of fluid flow, the effects of existence of bubbles or air in turbulent liquid flow on bubble velocity and bubble size distribution.

CHAPTER 2

LITERATURE REVIEW AND THEORY

Chapter 2 includes different kinds of literature reviews and theories related to the present research of this project. Some of the literature reviews involve experimental studies, theories, equipment and devices and numerical solutions. Section 2.1 on experimental studies provides an overview of other experiments conducted previously which contain the elements of interest with respect to this project. The results from these experiments are analyzed for further understanding. Section 2.2 on theories refers to all fundamental engineering or general knowledge regarding flow, bubbles, pipes and others. Some of the equipment and devices used by others, which are elaborated in Section 2.3, give more ideas on the improvement of the experiment setup. In Section 2.4, a related numerical simulation study is reviewed.

2.1 Experimental Studies

2.1.1 Bubble Size in Turbulent Air-water Flow through Horizontal Pipes

An experimental study is performed in a pipeline to evaluate the development of the bubble size distribution in the horizontal flow of an air–water system. As the air stream enters into the flowing water stream through a T-injector, it breaks into bubbles with a log-normal size distribution (Razzaque, 2003). Experiments are performed to determine bubble size distributions for three average water velocities for each of the three test section lengths. Three air volume fractions and two air injectors of different inner diameters are used. At large air volume fractions and small water velocities, the bubbles become highly deformed (Razzaque, 2003). From this experiment, T-injector gives a good choice of introducing bubbles into a liquid flow. Also, this project must be repeated with different water velocities and section lengths of pipes. Controlling bubble size can be done by using different air injectors of different inner diameters.

2.1.2 Bubble and Liquid Turbulence Characteristics of Bubbly Flow

In a work by Shawkat (2008), the bubble and liquid turbulence characteristics of air–water bubbly flow in a 200 mm diameter vertical pipe are experimentally investigated. The bubble characteristics are measured using a dual optical probe, while the liquid-phase turbulence was measured using hot-film anemometry. Measurements are performed at six liquid superficial velocities in the range of 0.2–0.68 m/s and gas

superficial velocity from 0.005 to 0.18 m/s, corresponding to an area average void fraction from 1.2% to 15.4% (Shawkat, 2008). From the experiment above, the gas velocity is always lower than the liquid velocity. This can be an important aspect to take care of during the experiment. Area average void fraction can be looked into to improve on this project.

2.1.3 Effect of Bubble Size in Turbulent Bubbly Downflow in a Vertical Channel

The effect of bubble size on the properties of downward turbulent flows of bubbly liquids in a vertical channel is examined. The turbulent channel flow is driven downward by an imposed constant pressure gradient (Lu and Tryggvason, 2007). Bubbles of two different sizes are introduced into the turbulent flow with a monodisperse or bidisperse distribution. The results show that for the cases studied here the bubble size has little effect on the void fraction distribution and the mean vertical velocity profile. The average velocity fluctuations and the vorticity profile across the channel do change (Lu and Tryggvason, 2007). To relate this experiment to the current project, downward turbulent flows of bubbly liquid in vertical channel can be considered as part of the experiments. Here, the bubbles only differ in two different sizes. A bigger range of bubble size should be considered in this project.

2.1.4 Bubbling Generation Technology and Application Using City Water Pressure

Another experiment is performed by Nakamura, Usuda and Morishita, 2007, where comparison and verification of the air-bubble effect against city water spouts is done with air-bubble generated by the co-developed nozzle. This nozzle is designed for water consumption volume and cost saving. The water flow volume has been controlled in all tests by adjustment of the opening or closing of two valves, using the same diameter nozzles, one is generating the air-bubble while the other is not. The outlet flow volumes are set to be 1.63, 6.10 and 10.00 L/min. The photos of both water flows with or without bubbles are taken by high speed digital camera with 2200 times/sec shutter speed, shown in Figure 2.1. The photos are then analyzed by the image analysis system and the water flow velocity can be calculated. The generated bubbles, as shown in Figure 2.2, the diameters are about 0.25-0.75 mm at the time of flow volume 1.3 L/min, 0.5-2.5 mm at the time of flow 2.7 L/min and 0.5-3.75 mm at the time of flow 3.3 L/min. From this

experiment, it is proven that by air-bubble in water spout, the flow speed is fast even with less water volume and the air-bubble diameter become bigger when the flow volume increases.

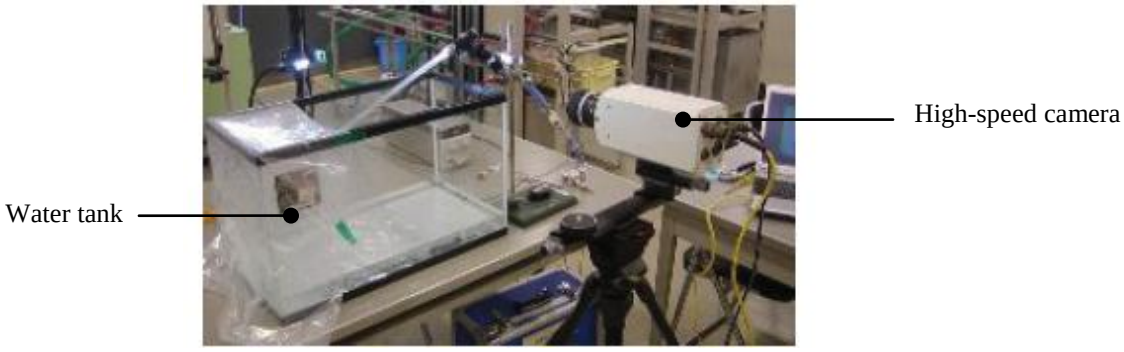

Figure 2.1: Measuring by high-speed camera (Nakamura et. al., 2007)

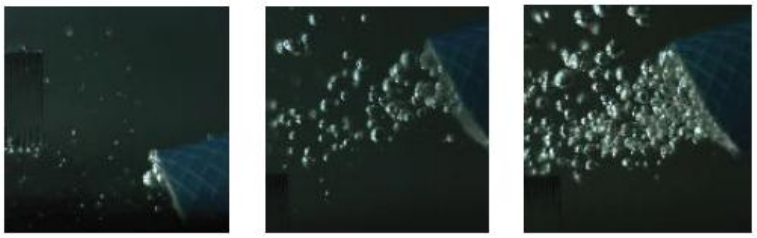

Figure 2.2: Different diameter ranges of bubbles generated by co-developed nozzle (Nakamura et al., 2007)

2.1.5 Visualization of the Flow around a Bubble Moving in a Low Viscosity Liquid

According to Lima-Ochoterena and Zenit (2003), the visualization of the streak lines is obtained by open-diaphragm photography of laser-sheet illuminated micro-tracers. The shape and position of the bubble is obtained, in the same photo plate, by simultaneously illuminating the flow with a stroboscopic light. This experiment is performed in a closed acrylic tank of 50×50×50 cm^3, in which bubbles are injected using a capillary tube. The schematic of experimental setup is shown in Figure 2.3. The working fluid here is filtered water while pure nitrogen is used to form the bubbles. In this experiment, a range of bubble sizes are used and the sizes are controlled by a fixed volume switch valve. The result from this experiment is a change of the bubble trajectory, from rectilinear to zig-zagging, as the volume increases.

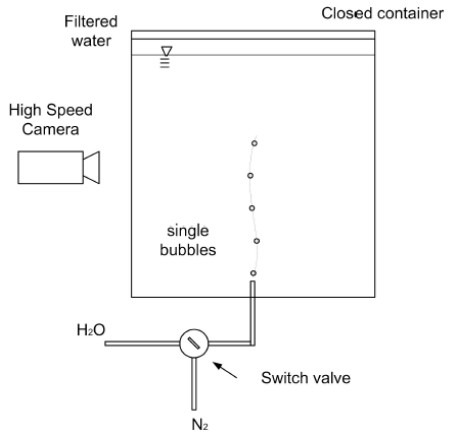

Figure 2.3: Schematic of experimental setup (Lima-Ochoterena and Zenit, 2003)

2.2 Theories

2.2.1 Disperse Flows

In disperse flows two types of models are available, trajectory models and two-fluid models. According to Bennen (2005), in trajectory models, the motion of the disperse phase is assessed by following either the motion of the actual particles or the motion of larger, representative particles. The details of the flow around each of the particles are subsumed into assumed drag, lift and moment forces acting on and altering the trajectory of those particles. The thermal history of the particles can also be tracked if it is appropriate to do so. Trajectory models have been very useful in studies of the rheology of granular flows primarily because the effects of the interstitial fluid are small. In the alternative approach, two-fluid models, the disperse phase is treated as a second continuous phase intermingled and interacting with the continuous phase. Effective conservation equations (of mass, momentum and energy) are developed for the two fluid flows; these included interaction terms modeling the exchange of mass, momentum and energy between the two flows. These equations are then solved either theoretically or computationally. Thus, the two-fluid models neglect the discrete nature of the disperse phase and approximate its effects upon the continuous phase. Inherent in this approach, averaging processes necessary to characterize the properties of the disperse phase; these involve significant difficulties. The boundary conditions appropriate in two-fluid models also pose difficult modeling issues (Brennen, 2005).

2.2.2 Natural or Forced Fluid Flow

A fluid flow is said to be natural or forced, depending on how the fluid motion is initiated. In forced flow, a fluid is forced to flow over a surface or in a pipe by external means such as a pump or a fan (Cengel and Cimbala, 2006). In natural flows, any fluid motion is due to natural means such as buoyancy effect, which manifests itself as the rise of the warmer (and thus lighter) fluid and the fall of cooler (and thus denser) fluid (Cengel and Cimbala, 2006). A flow field is best characterized by the velocity distribution, and thus a flow is said to be one-, two- or three-dimensional if the flow velocity varies in one, two or three primary dimensions, respectively. In this project, only two-dimensional flow is to be considered as it is easier to analyze.

2.2.3 The Control of Fluid Flow

To control the fluid flow through pipes, valves, for example gate valve and ball valve, are introduced. Pipe fittings for example elbow, tee, and reducer, are also used to assist in connections between pipes and suit designs of plants. When valve is open to allow full flow of liquid in a pipe connected to it as input, a rapid mixture of liquid and air originally in the pipe will occur and result in bubble formation. Bubbles in liquid flow could also be resulted by chemical processes in plant which have products of both liquid and gas phases as an outcome, for example the process of chlorination (Speight, 2001). Under these conditions where velocity is high enough, multiphase turbulent flow is produced. Liquid particle motion path is completely irregular that fluctuations of motion are very difficult to detect and only could be done by using laser (Sleigh, 2009). This indicates that a rapid variation of pressure and velocity in space and time occurs. With the mass and acceleration of fluid flow, forces are introduced and as the fluid travels along the pipe, work is done and high kinetic energy is created. With the forces and kinetic energy, vibration is induced. The existence of bubbles in liquid flow would create drag that leads to pressure drop. Pressure drop indicates energy loss and decrease in production rate.

2.2.4 Pressure Difference between Two Phases

The pressure difference between two phases is caused by three main effects: pressure differences due to surface energy of a curved interface, pressure differences due to mass transfer, and pressure differences due to dynamic effects (Corradini, 1997). In the first

case the simple existence of an interface (probably curved) requires from overall mechanical equilibrium that some pressure difference exist between the phases. This pressure difference is proportional to the interfacial surface tension and inversely proportional to the radius of curvature and is usually quite small in most applications. The second effect is noticeable when the mass flux due to phase change is large at the interface between the phases, for example large evaporation or condensation rates. The final effect is caused by dynamics where one phase has a larger pressure relative to the other phase due to very rapid energy deposition or pressurization effects.

2.2.5 The Development of Velocity Boundary Layer

At the entrance region of a circular pipe at a uniform velocity, because of no-slip condition, the fluid particles in the layer in contact with the surface of the pipe come to a complete stop. This layer causes the fluid particles in the adjacent layers to slow down gradually as a result of friction (Oertel and Prandtl, 2004). To make up for this velocity reduction, the velocity of the fluid at the midsection of the pipe has to increase to keep the mass flow rate through the pipe constant (Cengel and Cimbala, 2006). Thus, a velocity gradient develops along the pipe.

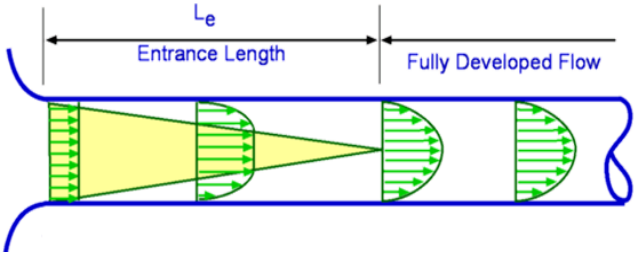

Figure 2.4: The development of the velocity boundary layer in a pipe for laminar flow (Cengel and Cimbala, 2006)

From Figure 2.4, the region from the pipe inlet to the point at which the boundary layer emerges at the centerline is called the entrance region, or hydrodynamic entrance region and the length of this region is called entrance length, L_e. Flow in the entrance region is called hydrodynamically developing flow since this is the region where the velocity profile develops. The region beyond the entrance region is fully developed and remain unchanged is called hydrodynamically fully developed flow (Oertel and Prandtl, 2004). The flow is said to be fully developed when the normalized temperature profile remains

unchanged as well. Pressure drop is directly related to the power requirements of the pump to maintain the flow. A pressure drop due to viscous effects represents an irreversible pressure loss and it is called pressure loss to emphasize that it is a loss (Cengel and Cimbala, 2006).

Having bubbles in turbulent flows can have significant effect on the wall drag. According to Murai (2007), it is difficult to create microbubbles and maintain them in the turbulent boundary layer, but wall drag can also be reduced by having small bubbles of a few milimetre in dimension. However, under some conditions, the wall drag can be increased with the presence of bubbles. A simulation of a bubbly channel flow conducted by Lu (2005) shows that drag is increased when bubbles travel close to the wall and this depends on the deformability and motion with respect to the wall. After that, another experiment is conducted to prove that pressure gradient is reduced more effectively compared to larger bubbles, typically larger than 5 mm, in vertical air-water upward flow containing small bubbles up to a few milimeters.

2.2.6 Sauter Mean Diameter

The drop size is the parameter most frequently used for the correlation of the combustion behaviour of an aerosol. If all drops in an aerosol are of the same size, then the obvious statement is that of droplet diameter. Such an aerosol is termed monosized or monodisperse. However, any fuel injection process such as atomization gives rise to a spectrum of different droplet sizes, in which the resultant droplet size distribution rarely fits the usual statistical functions (Lawes, 2004). Thus a form of averaging to determine a suitable mean size that properly represents the physical properties of droplets is necessary (Lefebvre, 1989). One of the commonly used mean sizes is the Sauter Mean Diameter (SMD), or D_{32}, which is given by

$$D_{32} = \frac{\sum_{i=1}^{k} n_i D_i^{\,3}}{\sum_{i=1}^{k} n_i D_i^{\,2}} \tag{2.1}$$

where, n_i is the number of droplets within a range centred on diameter D_i, and k is the number of ranges. The Sauter Mean Diameter is an average diameter with a volume to

surface area ratio equal to that of the droplets. It is an indicator of the degree of atomization produced by an injector.

Another representative of droplet diameters is the surface mean diameter, D_{20}, which represents an average diameter with a surface area equal to the mean surface area of all the droplets. This is given by:

$$D_{20} = \sqrt{\frac{\sum_{i=1}^{k} n_i D_i^{\,2}}{\sum n_i}} \tag{2.2}$$

The surface mean diameter is used for surface controlled applications such as absorption. Normally, a catalyst engineer will want to use D_{20} to compare the spheres on the basis of surface area because the higher the surface area the higher the activity of the catalyst (Rawle, 2005).

The mean arithmetic diameter is given by:

$$D_{10} = \frac{\sum_{i=1}^{k} n_i D_i}{\sum n_i} \tag{2.3}$$

Other mean droplet size terminologies have been defined in, for example, Schick (1997). For monodisperse or near monodisperse aerosols, all the mean droplet diameters tend to be the same. It is worth noting that, in the context of spray combustion, the use of mean diameters such as SMD to characterize flame instability may lead to mistaken conclusions since it is important to distinguish the homogeneity of the droplet spatial distribution.

Other than those mention above, a chemical engineer would want to compare spheres on the basis of weight. A number mean (number-volume or number-weight mean), which in mathematical terms is expressed as D_{30}, will be used. This is what is usually understood as the Volume Mean Diameter (VMD).

According to Rawle, (2005), academics normally prefer D_{43}, which is the volume moment mean of the particle, because the number of particles is not required. This would be inconvenient for any measurable size of find powder.

D_{32} is chosen to average the particle size of bubbles because it defines the diameter of a sphere that has the same volume/surface area ratio as a particle of interest. It is especially important in calculations where the active surface area is important, in this case, it is the active surface area of the bubbles in the water flow.

2.3 Equipment and Devices

2.3.1 Optical Investigation

One of the most popular classes of optical methods of investigation of flows is the class of so called "transillumination" methods in which the probing radiation is transmitted through the entire volume of the investigated inhomogeneity. Among them are all kinds of interferometry, including reference beam interferometry, shearing, holographic, Talbot, and speckle interferometry; the whole spectrum of shadow methods, from color-shadow methods to speckle interferometry; and probing of the investigated medium with the use of various laser sources, including spectrographs (Fomin, 2009).

From this literature review, the experiments for this project would be conducted on fluid flow with both vertical and horizontal pipelines rather than just one type. Data collected should be more scaled down for accuracy and precision. Gravitational acceleration should be taken into consideration for downward turbulent flows. The methods of introducing standard bubble sizes should be investigated whether they could be implemented at lab. With Laser Doppler Anemometry (LDA), velocity and turbulence at specific points in gas or liquid flow can be determined. While with Phase Doppler Analysis (PDA), the size and velocity of spherical particles can be measured simultaneously. Then, Dantec Dynamics' BSA Flow Software is used to obtain information like detailed droplet size and velocity measurements.

2.3.2 Experiments on the Effect of Acceleration on the Drag of Tap Water Bubbles

In an experiment done by van der Geld (2001), a special kind of bubble injection system, shown in Figure 2.5, is used to inject bubbles of different diameters all in micrometer. Air is supplied by two pressure reducers, two oil filters, a 5 µm filter and through a needle valve. From the figure, air (1) enters the inner capillary tube and leaves at the front orifice which has an inner diameter of 20 µm in a volume sheltered by a piece of plastic hose

(2). The diameter of the chamber is 2 mm and its length can be varied from 0 to 50 mm. At the downstream of the chamber, the second orifice is where the bubbles are created. The diameter available for this orifice is 30, 40, 50, 60, 80, 110 or 150 µm. This depends on the flow conditions. The bubble generating frequency is regulated by adjusting the volume and the pressure at the chamber. After the detachment of a bubble, the chamber has to be pressurized again before a new bubble can be formed.

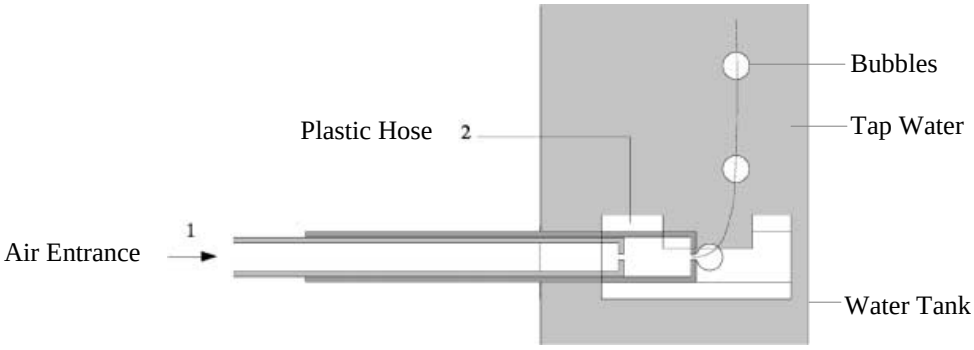

Figure 2.5: Schematic of variable chamber bubble injector (van der Geld, 2001)

2.3.3 Velocity Measurements of Liquid and Gaseous Phase of Bubbles Rising in Water

Another way of generating bubbles is by using a bubble swarm generator in Figure 2.6. This system comprises of seven individual bubble generators. The generators release defined portions of pressurized air via two magnetic valves. In order to have a reproducible volume of air to generate a single bubble, two valves are arranged in series and at a short distance apart. A rough variation of bubble size is achieved by controlling through the valves up to an overlap of the opening times. Fine control of bubble size can also be accomplished by varying the upstream air pressure. To make sure that air bubbles generated are separated and do not collapse, air is ejected through a nozzle with very small opening and high pressure drop into a capillary of larger diameter. This variation in air pressure results in bubbles produced with diameter range of 4.0-7.0 mm (Lindken and Merzkirch, 2000).

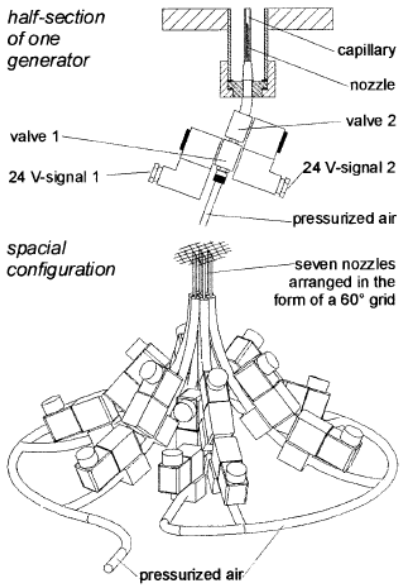

Figure 2.6: Bubble swarm generator (Lindken and Merzkirch, 2000)

2.4 Numerical Simulations

A CFD simulation of a cavitation model is used to study the cavitation in an automotive fuel pump by Xing and Hadzic in 2004. Automotive fuel pumps are devices used to draw fuel from a vehicle's tank into the fuel system. The pump entrains a fuel-vapor mixture through the inlet, and the model accounts for condensation and also localized cavitation. Experimental measurements are used to predict mass flow rate as a function of pressure drop across the pump. This model is important in order to evaluate pump performance across several operating conditions, including near vapor lock conditions, where blockage in the fuel delivery occurs due to vapor bubbles. These vapor bubbles are believed to be generated by excess cavitation. The values for this model are chosen at the inlet and outlet so that a fixed pressure rise across the pump could be maintained. The predicted flow rates are then compared with experimental measurements made by the manufacturer. The CFD results are in agreement with experiment. CFD analyses provide insight into the flow patterns inside the pump, which can then be used to illustrate the impact of certain geometric features on the pump performance. Figure 2.7 shows the modeling of the fuel pump geometry by using the CFD.

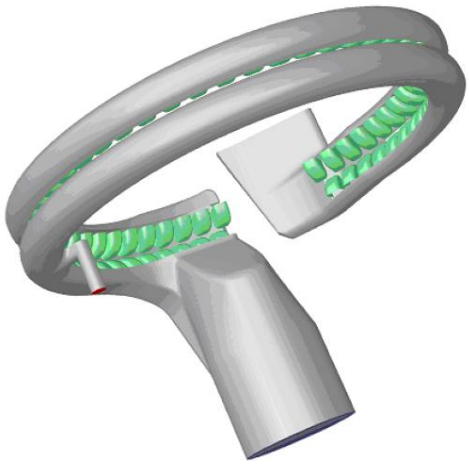

Figure 2.7: The FLUENT fuel pump geometry (Xing and Hadzic, 2004)

CHAPTER 3

METHODOLOGY

This chapter includes a set of methods or procedures which provides the description of the schedule of the project. In Section 3.1, the Gantt chart and project milestones are presented.

Project process flow is presented in Section 3.2, which illustrates the work sequence of the project, from the start until the end.

3.1 Gantt Chart and Milestones

The activities or work done during the first semester are listed out and the total period of time involved are fourteen weeks. Selection of project topic and preliminary research work were done within the period planned. Research and literature review are carried out from week 5 until week 14 for more understanding of the project. Literature review was done on variety sources for example journals, articles, researches, conferences, webpages and others. In weeks 5 and 6, an experimental work was carried out using a cavitation pump rig as an introduction to the project work. The equipment was modified in order to meet the objective of the project. The modification involved a portion of pipe of the equipment. However, the process of modification could not be carried out within the period of time planned. This was due to some obstacles in finding spare parts and carrying out mechanical work.

Table 3.1 gives a clear illustration on the schedule of this project for activities done in the first semester. Introduction of Laser Doppler Anemometry (LDA) was done at an LDA lab. A briefing about the working priciples and functions of LDA was attended. The cavitation pump rig was transferred to the LDA lab, which was located at a different building, for data collection using the LDA.

Table 3.1 Gantt chart and milestone for activities in Semester I

No.	Activities/Work	1	2	3	4	5	6	7	8	9	10	11	12	13	14
1	Selection of project topic														
2	Preliminary research work														
3	Research and literature review														
4	Introduction of cavitation pump rig														
5	Modification of cavitation pump rig if needed														
6	Familiarization with cavitation pump rig														
7	Introduction of LDA/PDA														
8	Experimental work on Laser Doppler Anemometry (LDA)														
9	Submission of preliminary report					●									
10	Submission of progress report								●						
11	Seminar								●						
12	Submission of interim report final draft														●
13	Oral presentation														●

Legend: Planned
Completed
Milestones

Table 3.2 is an illustration of the progress of the second part of this project. In the second semester of this project, the transportation of cavitation pump rig to the LDA/PDA lab was done within the first two weeks. Research and literature review was carried out throughout the semester, which was from week 2 until week 13. The combination of cavitation pump rig with LDA/PDA was done for further investigation of this project. Adjustment of both equipment was performed to obtain the desired position for the laser beam to be aligned at the correct measurement points in the pipe. From there, data collection could be done and experimental work was repeated to obtain data for water with bubbles flowing vertically upward. The experimental work was completed on time as planned, which was in week 9.

Table 3.2 Gantt chart and milestone for activities in Semester II

No.	Activities/Work	1	2	3	4	5	6	7	8	9	10	11	12	13	14
1	Transportation of cavitation pump rig to LDA/PDA lab														
2	Research and literature review														
3	Combination of cavitation pump rig and LDA/PDA														
4	Experimental work and data collection														
5	Submission of Progress Report 1				●										
6	Submission of Progress Report 2								●						
7	Seminar								●						
8	Poster Exhibition										●				
9	Submission of Dissertation Final Draft														●
10	Oral Presentation	During study week													
11	Submission of Dissertation (hard bound)	7 days after oral presentation													

Legend: Planned
Completed
Milestones

3.2 Project Process Flow

Shown in Figure 3.1 is the process flow of the project. The process involved in the project includes the choice and submission of titles and preliminary research work to get more exposure on the title of project. An introduction to the equipment, cavitation pump rig, was conducted by running the equipment without introducing bubbles to the water flow in pipe. The sequence of manually operating the equipment was learned and practiced so as to familiarize the equipment. Then, a briefing for Laser Doppler Anemometry (LDA)/Phase Doppler Anemometry (PDA) was conducted to introduce the parts of the equipment and the basic working principles. After knowing the working principles of the equipments, bubble injection method was created to support the mechanism of introducing micron bubbles into the pump system.

A modification of the pipe was needed in order to keep the water flow meter in place while conducting experiments. To create bubbles in the cavitation pump system, a hole was punctured at the pipe and bubbles were injected with an air pump.

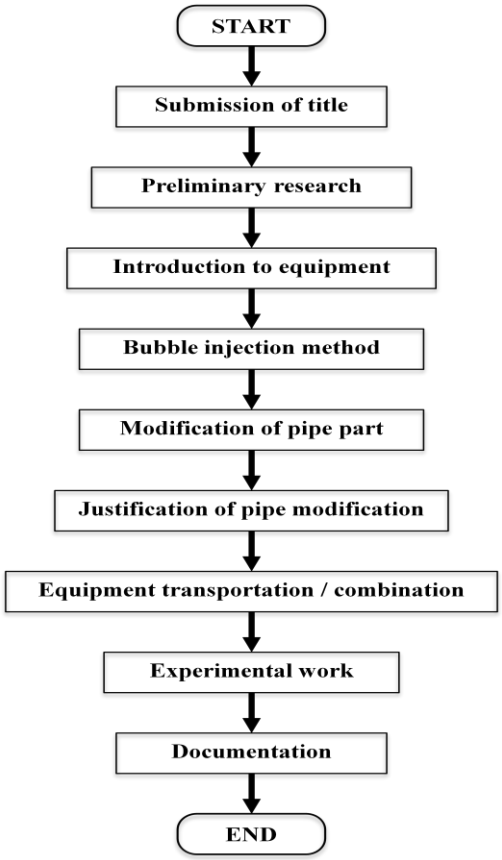

Figure 3.1: Process flow diagram of the project

After that, the cavitation pump rig was ready to be transported to the LDA/PDA lab. This was for the ease of combining the cavitation pump rig with the LDA/PDA equipment. The cavitation pump rig serves the function of producing bubbly flow in transparent pipe while the LDA/PDA transmits laser beams which will hit the bubbly flow in the pipe and generates desired data (diameter, vertical velocity and horizontal velocity of bubbles). Due to the limitation of the LDA/PDA in terms of horizontal and vertical displacements, the laser could only hit certain pipe parts of the cavitation pump rig. Thus, a decision was made to neglect the water flow rate and bubble injection would be done through the quick release connector which was originally placed after the pump. Experiments were then conducted for 3 different elevation and 4 points across the pipe at each elevation. Data acquired contained bubble diameter in micron meter and also vertical velocity and horizontal velocity in meter per second. After experiments were finished, the cavitation pump rig was transported back to the original place. Poster was prepared for exhibition after that. Documentations were finalized and the project is complete.

CHAPTER 4

EXPERIMENT SETUP

A description of experiment setup is explained in this chapter in detail. This includes the details of equipments used to conduct experiments, namely cavitation pump rig and Laser Doppler Anemometry (LDA)/Phase Doppler Anemometry (PDA). Specification, orientation and illustration are shown in this chapter for every element of the equipments. The modification of cavitation pump rig is explained in detail. A few trials of experiments using water spray are also included in this chapter.

4.1 Cavitation Pump Rig

Cavitation pump rig, as shown in Figure 4.1, serves the function of pumping water (normal pipe water) from the water tank which will then flow through the pipe system (transparent) and back to the water tank. Bubbles are introduced to the water flow to create bubbly flow. The transparent pipe system is the most important element as the transparency allows the laser to penetrate through the pipe wall and reach the bubbly flow inside the pipe. With this, the laser beam could be transmitted to the desired area of interest and laser signals could then be received and transmitted to the software for further analysis. The main components of cavitation pump rig are water pump, pipe system and water tank.

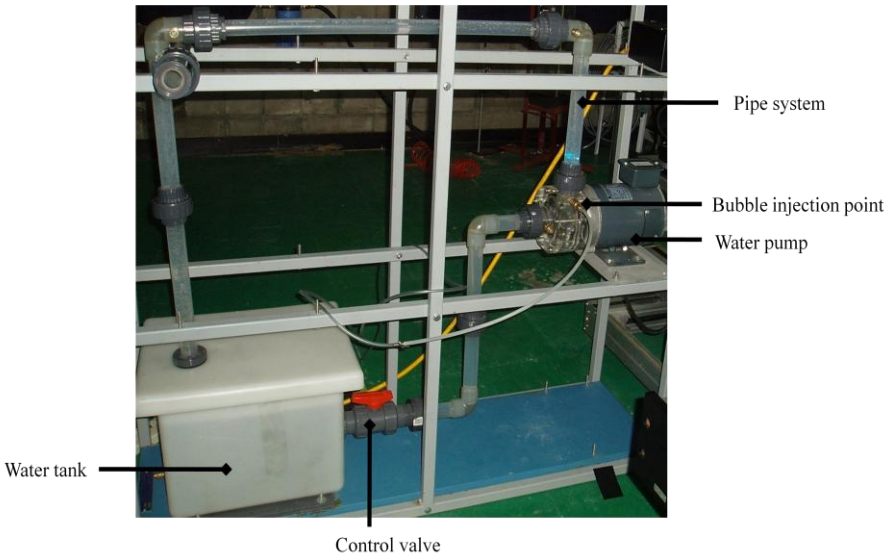

Figure 4.1: Cavitation pump rig

The schematic diagram of cavitation pump rig is illustrated in Figure 4.2.

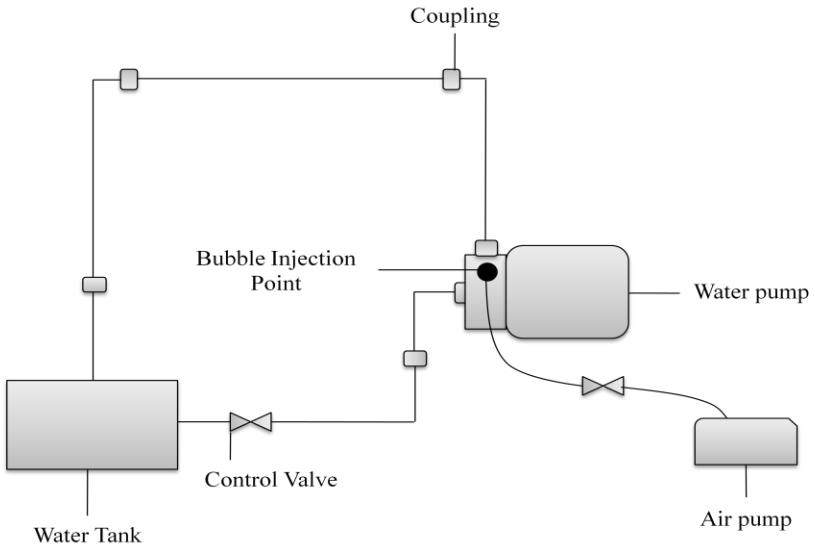

Figure 4.2: Schematic diagram of cavitation pump to be used with LDA/PDA

The water in the pump system flows in a circulation. Figure 4.3 shows the water circulation in the cavitation pump rig. Water is sucked up by the water pump from the water tank, through the control valve and rotor blade. The water flows up vertically along the pipe system and then goes back to the water tank. Bubbles injected are carried upward by the flowing water.

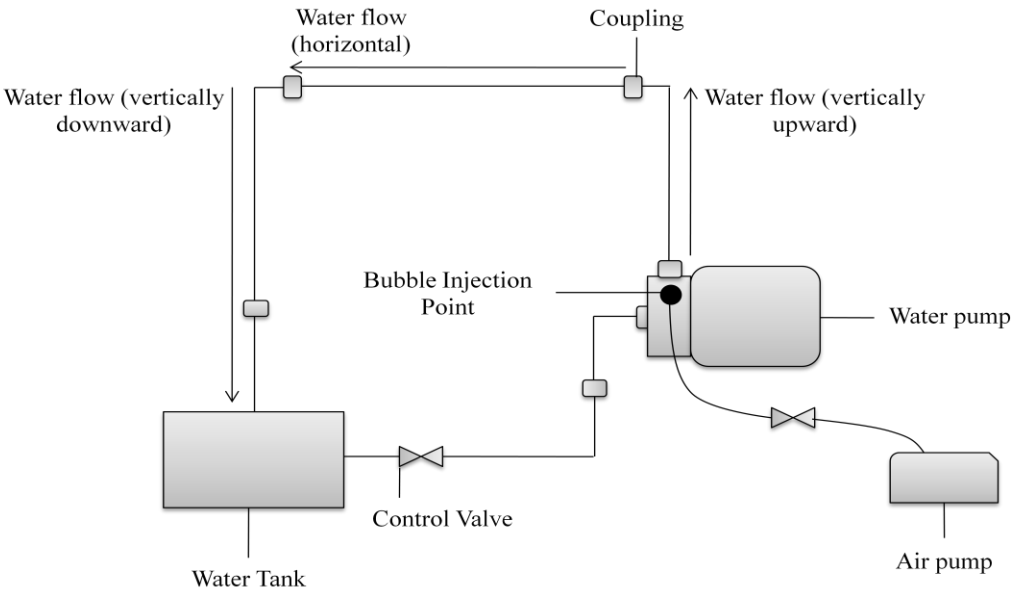

Figure 4.3: Water circulation in cavitation pump rig

4.1.1 Water Pump

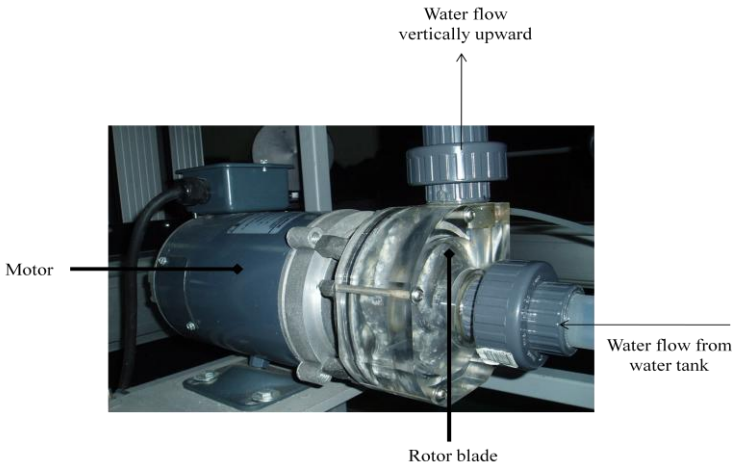

Figure 4.4: Water pump

Figure 4.4 shows the water pump, which consists of a motor and a rotor blade, functions as a device to pump up the water from a water tank which is located at a lower elevation to fill up the whole pipe system of the pump rig. The water then is circulated back to the water tank. This water circulation is continuous and the speed of motor is controlled by a DC motor speed control, which is shown in Figure 4.5. The scale on the controller to indicate the motor speed is %rpm.

The specifications of the water pump are:

- Full rpm: 1725 rpm
- Voltage: 90 V
- Current: 3 A

Figure 4.5: DC motor speed control

4.1.2 Air Pump

Figure 4.6: Air pump

Figure 4.6 shows the air pump used for this project to introduce bubbles into the water flow in pipe. The tubing is used to channel compressed air from the air pump to the quick release connector at cavitation pump rig. Maximum velocity of this air pump is 1.50 m/s and it is used throughout the experiments. The mechanism is shown in Figure 4.7.

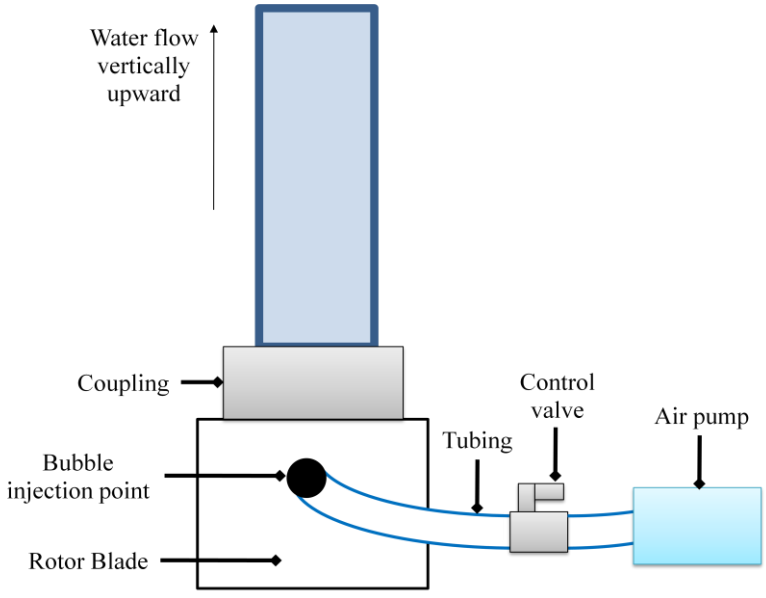

Figure 4.7: The introduction of bubbles using air pump

The compressed air flow from the air pump is controlled by an air flow valve. Figure 4.8 shows the condition of the air flow valve when it is fully open. In this project, the air flow rate is a constant variable. Full volume of air flow is used for all experiments conducted.

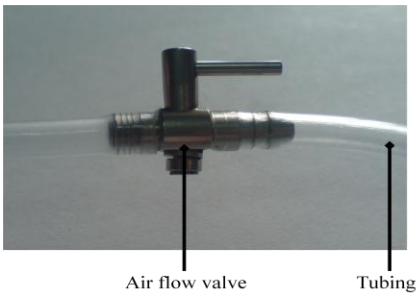

Figure 4.8: Air flow valve

4.1.3 Pipe System

The transparent pipes are made of plastic and are joined by couplings with polyvinyl chloride (PVC) material. Leakages between the joints are prevented by O-rings.

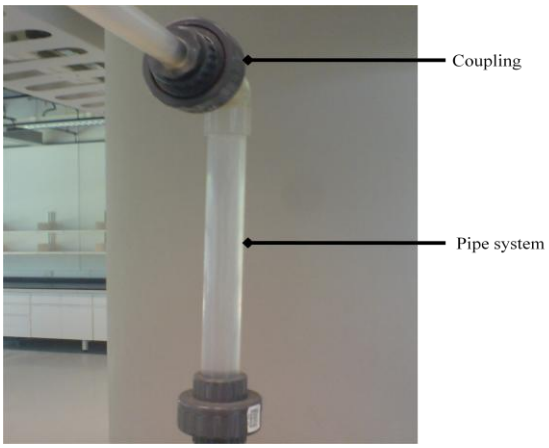

Figure 4.9: Pipe elbow

Figure 4.9 shows an elbow of the pipe system. Data collection will be carried out for only one pipe part. The position of the pipe part is illustrated in Figure 4.10.

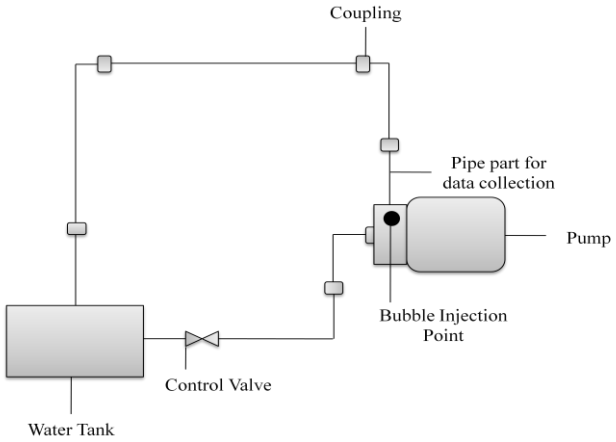

Figure 4.10: Position of the specific pipe part for data collection

The specification of the pipe part is illustrated in Figures 4.11 and 4.12.

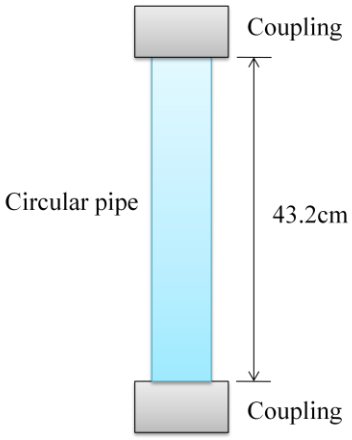

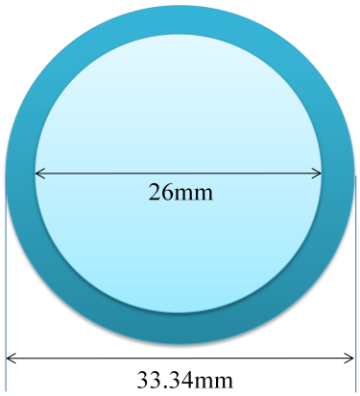

Figure 4.11: Pipe length

Figure 4.12: Pipe inner and outer diameter

The flow rate of water will be indicated by the water flow meter. Figure 4.13 shows the water flow meter used in this experiment. The water flow rates are determined first before the experiments are conducted. The unit for the water flow rate is gallon per minute (gpm). The minimum water flow rate is 1 gpm while the maximum water flow rate is 23 gpm.

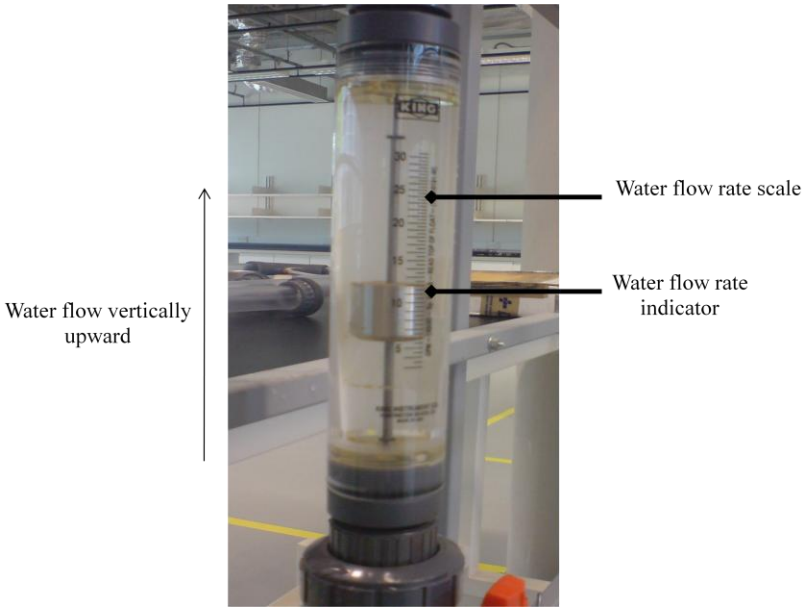

Figure 4.13: Water flow meter

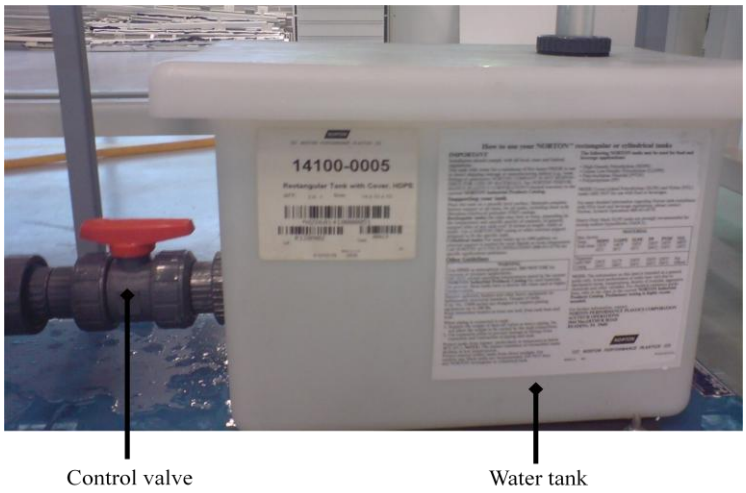

Figure 4.14: Control valve

Figure 4.14 shows a control valve (ball valve type) placed in between the tank and water pump to control the flow of water from the tank to the pump and prevent too much reverse flow when the pump is switched off. This will help ease the start up of the whole system for the next time.

4.1.4 Modification of Pipe

A modification of the pipe is needed in order to keep the water flow meter in place while conducting experiments. To create bubbles in the cavitation pump system, a hole is punctured at the position illustrated in Figure 4.15.

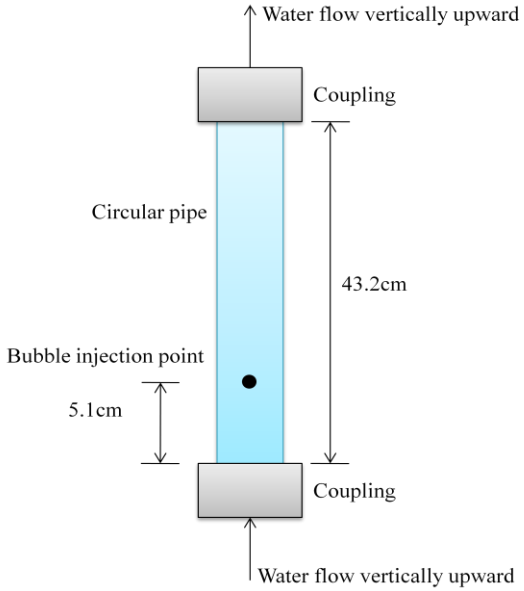

Figure 4.15: Bubble injection point at modified pipe part

The original pipe part is replaced by the modified one and experiment is therefore conducted for trial. Figure 4.16 shows the replacement of modified pipe part and the orientation of the cavitation pump system.

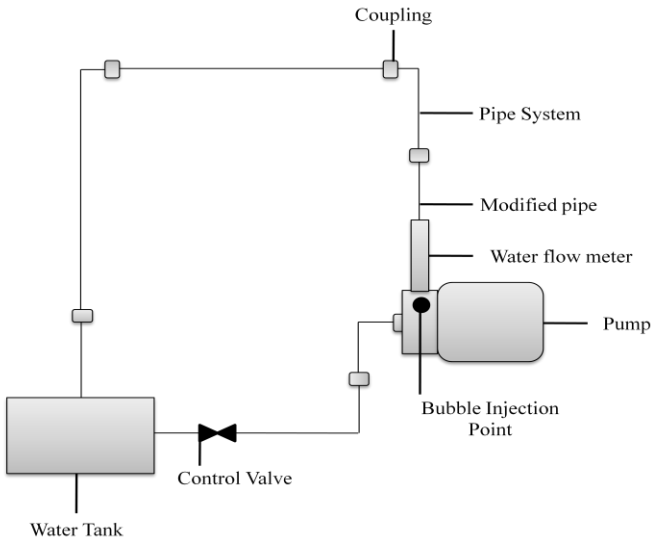

Figure 4.16: The replacement of modified pipe part and cavitation pump system orientation

However, this orientation needs to be redesigned as there are constraints due to the orientation of LDA/PDA. The modified pipe part together with the water flow meter is neglected for all the experiments conducted. This will lower the position of the pipe from which the data will be collected. The orientation on the cavitation pump rig modified due to the constraints of LDA/PDA is illustrated in Figure 4.17.

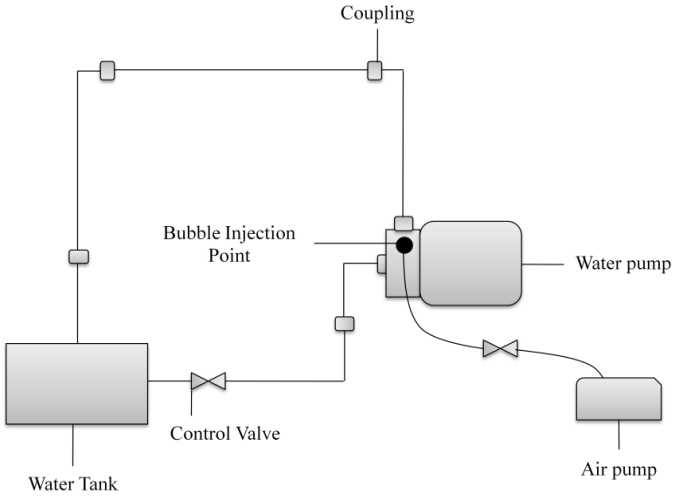

Figure 4.17: Modified cavitation pump rig due to the constraints of LDA/PDA

4.2 Laser Doppler Anemometry/Phase Doppler Anemometry

4.2.1 Laser Doppler Anemometry

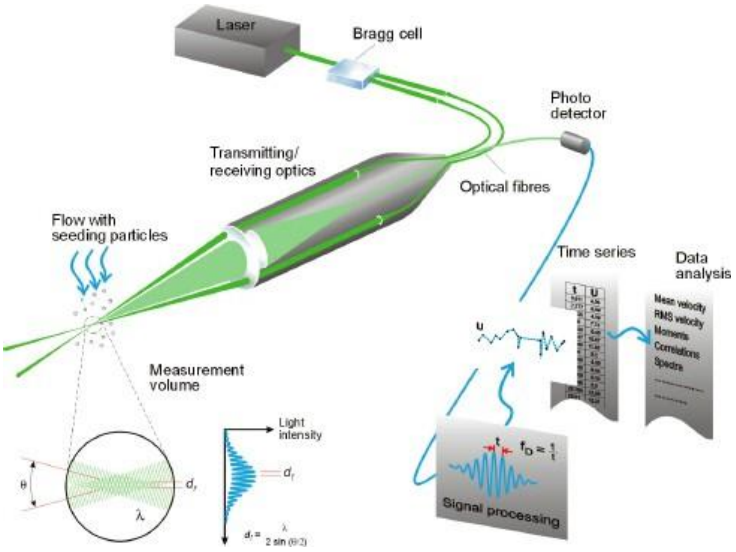

Figure 4.18: Laser Doppler Anemometry (Dantec Dynamics, 2010)

In Figure 4.18, Laser Doppler Anemometry (LDA) is shown a non-intrusive optical technique used to measure velocity and turbulence at specific points in gas or liquid flows. Applications of LDA include measurements of free flows around road vehicles, aircrafts and ships and internal flows in pump, mixers, turbines and engines. Measurements improve knowledge about the flow and can lead to better efficiency and reduced noise. With this equipment the movement of the air bubbles that have very small diameter, normally in micron can be investigated. Data for vertical velocity, horizontal velocity and diameter of the air bubbles could be obtained.

The basic configuration of an LDA consists of:

- A continuous wave laser
- Transmitting optics, including a beam splitter and a focusing lens
- Receiving optics, comprising a focusing lens, an interference filter and a photo detector
- A signal conditioner and a signal processor.

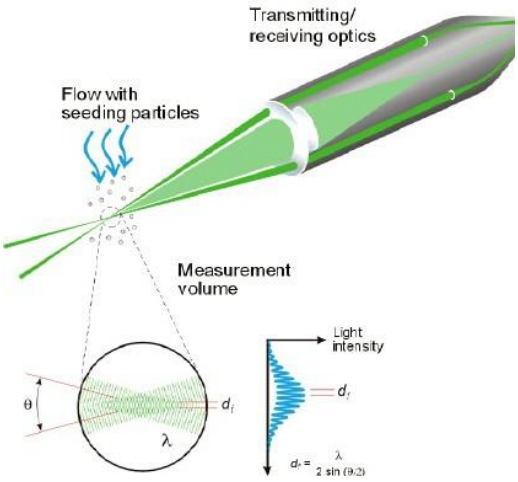

Figure 4.19: The probe and the probe volume

Figure 4.19 shows the probe volume. The probe volume is typically a few millimeters long. The light intensity is modulated due to interference between the laser beams. This produces parallel planes of high light intensity, so called fringes. The fringe distance d_f is defined by the wavelength of the laser light and the angle between the beams:

$$d_f = \frac{\lambda}{2 \sin(\theta/2)} \tag{4.1}$$

Each particle passage scatters light proportional to the local light intensity. Flow velocity information comes from light scattered by tiny "seeding" particles carried in the fluid as they move through the probe volume. The scattered light contains a Doppler shift, the Doppler frequency f_D, which is proportional to the velocity component perpendicular to the bisector of the two laser beams, which corresponds to the x axis shown in the probe volume. The scattered light is collected by a receiver lens and focused on a photo-detector. An interference filter mounted before the photo-detector passes only the required wavelength to the photo-detector. This removes noise from ambient light and from other wavelengths.

The photo-detector converts the fluctuating light intensity to an electrical signal, the Doppler burst, which is sinusoidal with a Gaussian envelope due to the intensity profile of the laser beams. The Doppler bursts are filtered and amplified in the signal processor, which determines f_D for each particle, often by frequency analysis using the robust Fast Fourier Transform algorithm. The fringe spacing, d_f provides information about the distance travelled by the particle.

The Doppler frequency, f_D provides information about the time:

$$t = \frac{1}{f_D} \tag{4.2}$$

Since velocity equals distance divided by time, the expression for velocity thus becomes:

$$V = d_f \times f_D \tag{4.3}$$

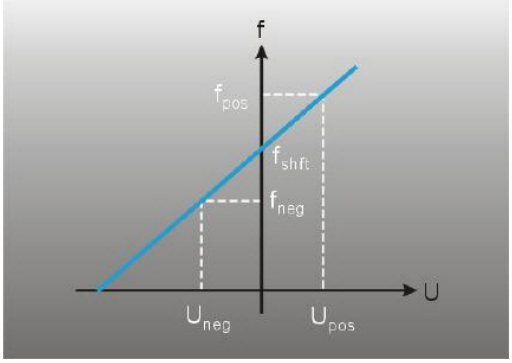

Figure 4.20: Doppler frequency to velocity transfer function for a frequency shifted LDA system

Figure 4.20 shows the determination of the sign of the flow direction. The frequency shift obtained by the Bragg cell makes the fringe pattern move at a constant velocity. Particles which are not moving will generate a signal of the shift. LDA systems without frequency shift cannot distinguish between positive and negative flow direction or measure zero velocity. LDA systems with frequency shift can distinguish the flow direction and measure zero velocity.

In Figure 4.21, to measure two velocity components, two extra beams can be added to the optics in a plane perpendicular to the first beams. All three velocity components can be measured by two separate probes measuring two and one components, with all the beams intersecting in a common volume as shown below. Different wavelengths are used to separate the measured components. Three photo-detectors with appropriate interference filtres are used to detect scattered light of the three wavelengths.

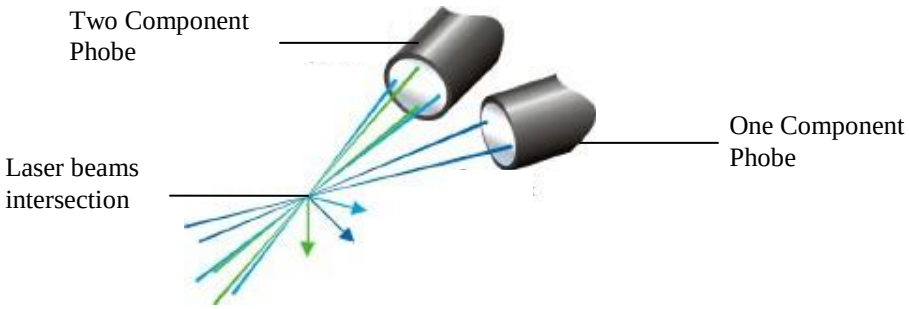

Figure 4.21: Beams added to the optics in a plane perpendicular to the first beams to measure two velocity components (Dantec Dynamics, 2010)

4.2.2 Phase Doppler Anemometry

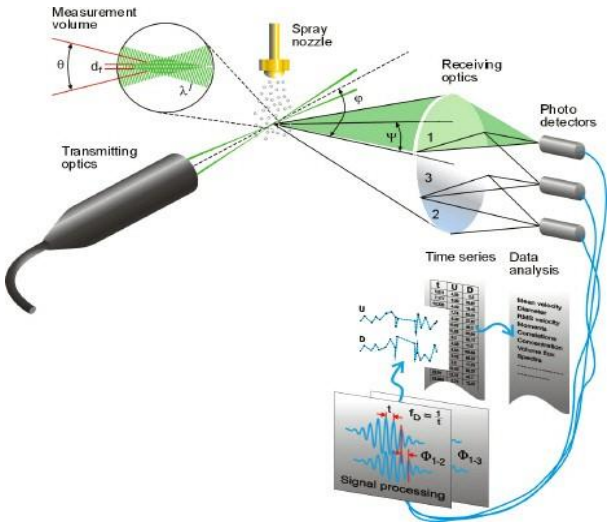

Figure 4.22: Phase Doppler Anemometry (Dantec Dynamics, 2010)

As shown in Figure 4.22, Phase Doppler Anemometry (PDA) is an optical technique to measure the size and velocity of spherical particles simultaneously. These particles can be droplets, bubbles or solid particles, as typically occur in sprays, liquid atomization, bubbly two-phase flows and multiphase flows with, for example, glass beads. The measurement point is defined by the intersection of two focused laser beams and the measurements are performed on single particles as they move through the sample volume. Particles thereby scatter light from both laser beams, generating an optical interference pattern.

A receiving optics placed at a well-chosen off-axis location projects a portion of the scattered light onto multiple detectors. Each detector converts the optical signal into a

Doppler burst with a frequency linearly proportional to the particle velocity. The phase shift between the Doppler signals from different detectors is a direct measure of the particle diameter.

The particle velocity U is calculated from the Doppler frequency f_D of the signal from any one of the detectors:

$$U = \frac{\lambda}{2\sin(\frac{\theta}{2})} f_D \tag{4.4}$$

The particle size D is derived from the phase difference F between the signals from two detectors. If light scattering is dominated by reflection:

$$\Phi = \frac{2\pi D}{\lambda} \frac{sin\theta sin\psi}{\sqrt{2(1-cos\theta cos\psi cos\phi)}} \tag{4.5}$$

If light scattering is dominated by refraction:

$$\Phi = \frac{-2\pi D}{\lambda} \frac{\eta_{rel} sin\theta sin\psi}{\sqrt{2(1+cos\theta cos\psi cos\varphi)(1+\eta_{rel}^2-\eta_{rel}\sqrt{2(1+cos\theta cos\psi cos\varphi)})}} \tag{4.6}$$

In Figure 4.23, the maximum particle size that can be unambiguously measured with two detectors corresponds to a phase shift of $F_{1\text{-}2}$ = 360°. Reducing the distance between the detectors can extend the particle size range. This however, will also reduce the measurement resolution. Using three detectors provides both a large measurable size range ($F_{1\text{-}3}$) and a high measurement resolution ($F_{1\text{-}2}$).

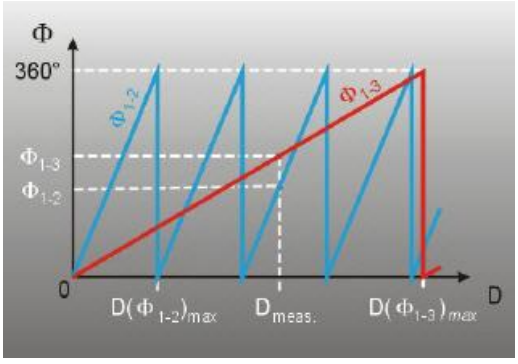

Figure 4.23: Light scattering, Φ versus particle size, D

4.2.3 Integrated PDA Solutions

Dantec Dynamics' Particle Dynamics Analysis (PDA) systems measure on-line the size, velocity and concentration of spherical particles, droplets or bubbles suspended in gaseous or liquid flows. The principles of Particle Dynamics Analysis (PDA)

1. The measurements are performed at the intersection of two laser beams, where there is an interference fringe pattern of alternating light and dark planes.
2. Particles scatter the light, which appears to flash, as the particles pass through the bright planes of the interference pattern. Receiving optics placed at an off-axis location focus scattered light onto multiple detectors.
3. Each detector converts the optical signals into a Doppler burst with a frequency linearly proportional to the particle velocity.
4. The processor measures the phase difference between the Doppler signals from different detectors. This is a direct measure of the particle diameter.
5. Results are processed by the BSA Flow Software Packages.

4.2.4 LDA/PDA Orientation in UTP Lab

Figure 4.24 shows the orientation of the LDA/PDA lab in Universiti Teknologi PETRONAS (UTP). The laser source is shown in Figure 4.25.

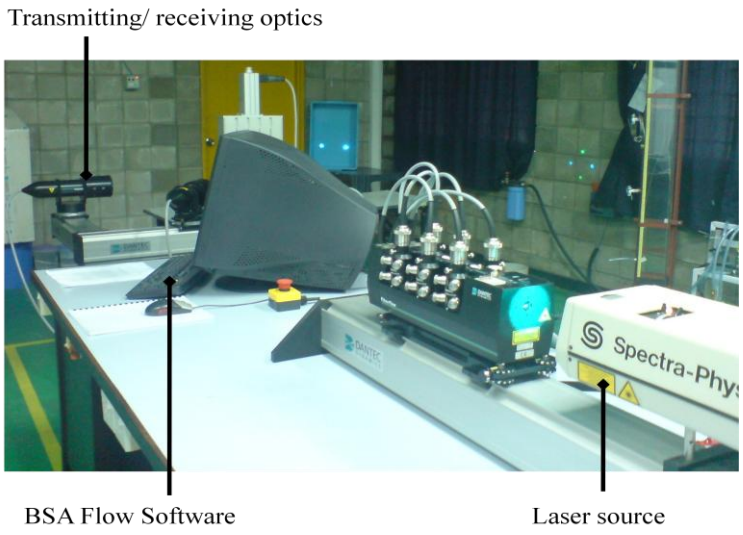

Figure 4.24: LDA/PDA orientation in UTP lab

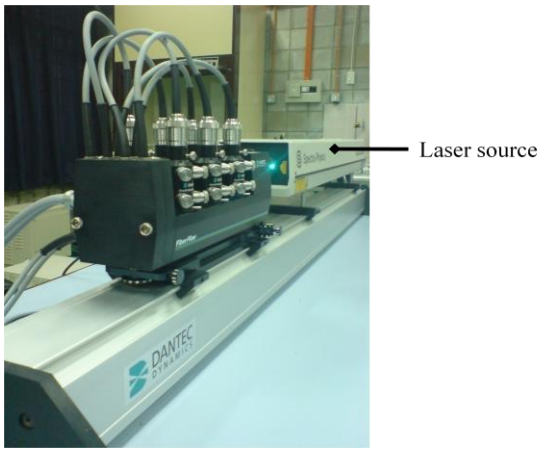

Figure 4.25: Laser source for LDA/PDA

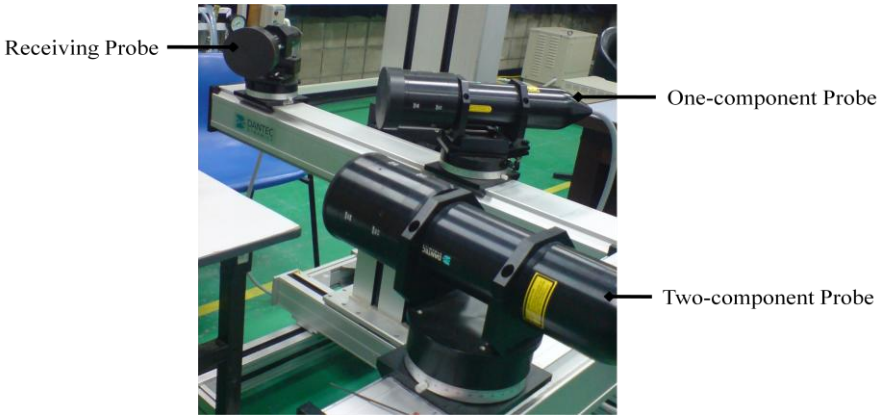

Figure 4.26: Transmitting and receiving probes

Figure 4.26 shows the orientation of transmitting and receiving probes. There are two transmitting probes, which are one-component probe and two-component probe. For this project, only two-component probe is taken into consideration for 2-D results. There are 4 laser beams transmitted from the laser source which then converge to form an intersection point. As for the one-component probe, which will give 3-D results, is neglected. The receiving probe takes in laser signals from the intersection point and transmits them to the BSA software (from the computer) to be interpreted.

4.3 Vane Anemometer

A vane anemometer is a device that measures the velocity of the air or wind, as well as air pressure (Hale, 2009). The vane anemometer used in this project is called handheld anemometer and was used to take measurement of velocity of the air flow from the air pump. The maximum velocity of air injected into the pipe is 1.50 m/s. Figure 4.27 shows

the vane anemometer set used in this project to measure the velocity of the air pumped into the pipe system in order to induce air bubbles.

Figure 4.27: Vane anemometer set

4.4 Experiment Setup

4.4.1 Laser Beam Intersection

Before LDA/PDA was combined with cavitation pump, the laser beam intersection point must be identified and marked so that the data points could be easily adjusted in place after that. In Figure 4.28, the four laser beams are shown. The beams were transmitted by the two-component probe and converged into a single intersection point.

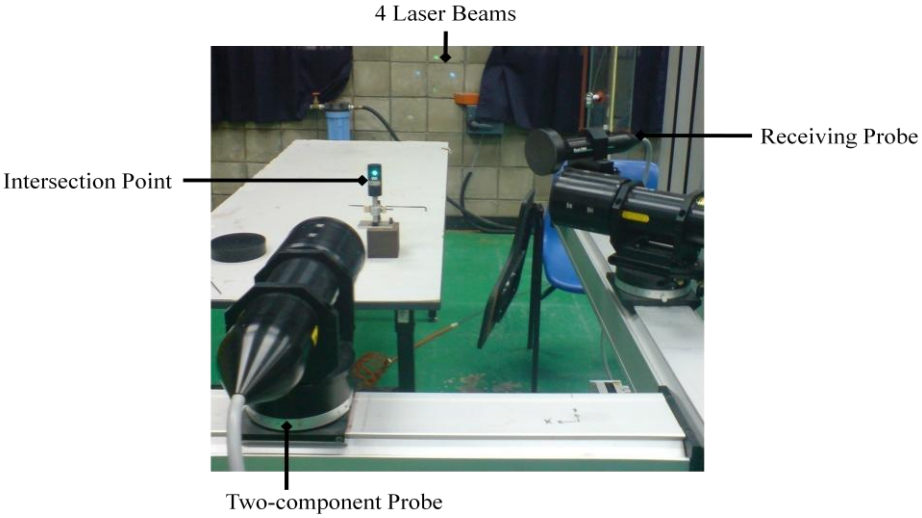

Figure 4.28: Laser beam intersection

4.4.2 Experiment Trial using Water Spray

An experiment trial was conducted by using the water spray. This was to make sure that the intersection point found was at the right position and to test run the software. With water spray experiment as trial, it was confirmed that the LDA/PDA system and BSA Flow Software Packages were at the perfect conditions to be used. The setup of the experiment trial is shown in both Figure 4.29 and Figure 4.30.

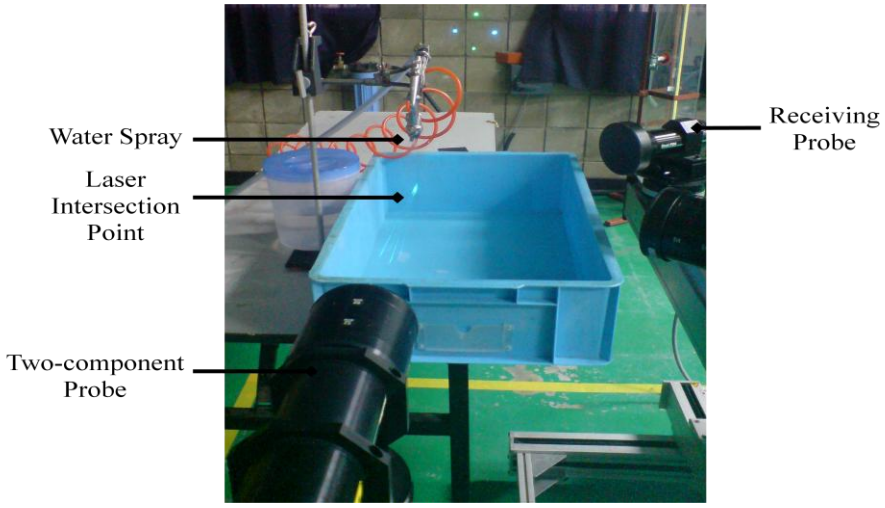

Figure 4.29 Experiment trial using water spray

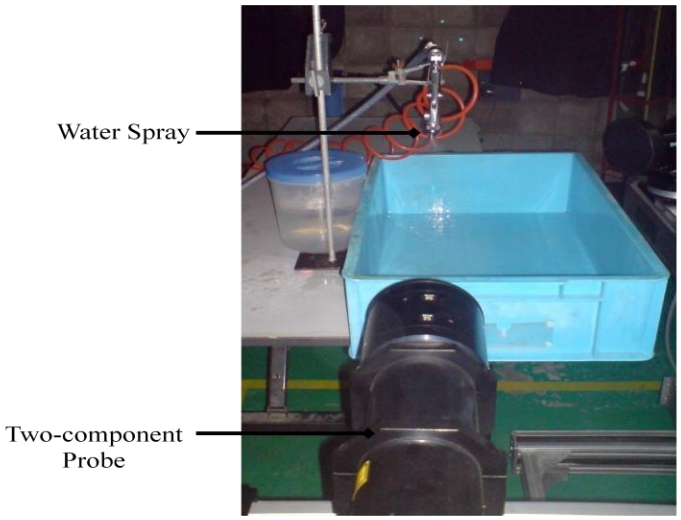

Figure 4.30 Experiment trial using water spray

4.4.3 Combination of LDA/PDA and Cavitation Pump

It is shown in Figure 4.31 that the combination of LDA/PDA and Cavitation Pump is done before the experimental work could be conducted for further investigation. This included the transportation of the equipment and adjustment of the position of the pipes and the transmitting and receiving probes.

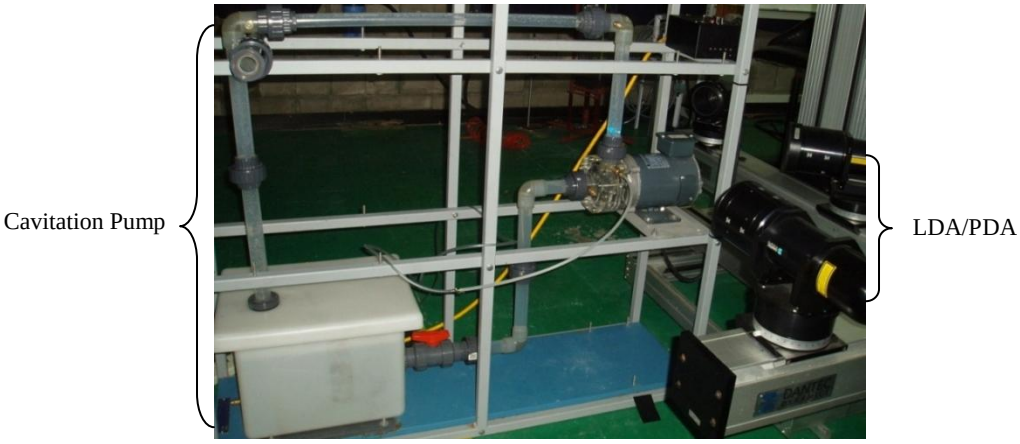

Figure 4.31: Combination of cavitation pump and LDA/PDA

4.4.4 Bubble Injection and Laser Beam Intersection Point

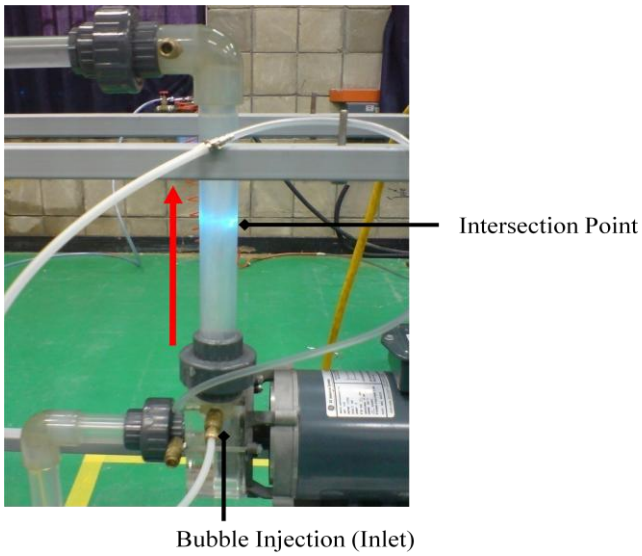

Figure 4.32: Laser beams intersect inside pipe with bubble injection at the inlet

Figure 4.32 shows that the laser beams intersected inside the pipe. The position of the laser and the pipe was estimated by the marking of the intersection point earlier on.

4.4.5 Data Acquisition

Data collection was done at 12 different points of different height and displacement from the pipe. The positions of the data points are illustrated in Figure 4.33. The exact coordination of the data points are shown in Figure 4.34.

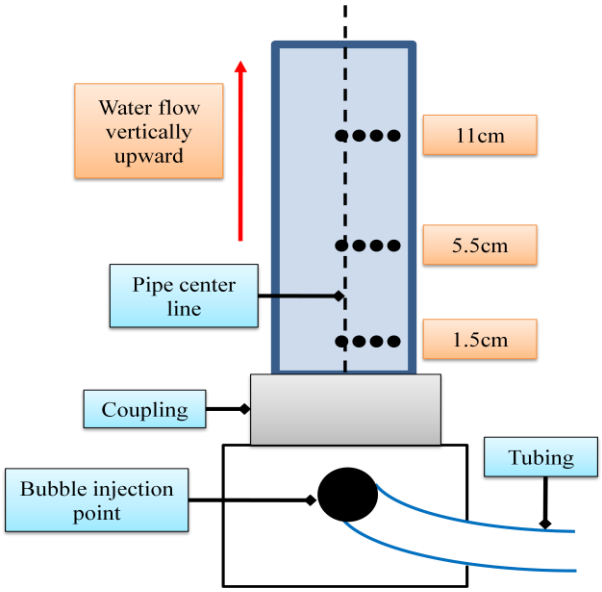

Figure 4.33: The positions of the points for data collection

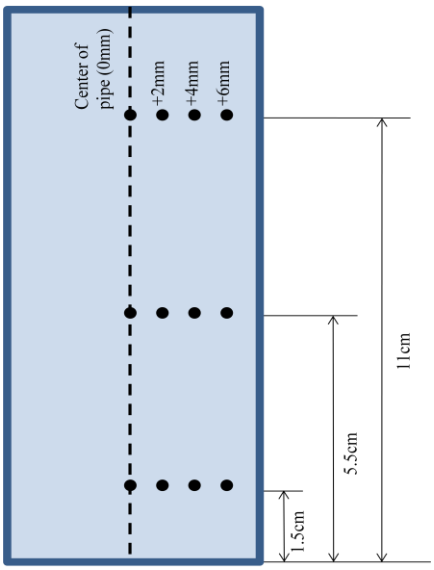

Figure 4.34: Coordination of data points

4.4.6 BSA Flow Software Data Sheet

BSA Flow Software data sheets were obtained for further analysis. It is displayed on the monitor screen once the receiving probe has received enough data to be tabulated into histogram. Figure 4.35 shows a data sheet example for 5 gpm water flow rate at an elevation of 1.5 cm from the coupling at the center of pipe. The counts on the y-axis represent the number of counts × 1000.

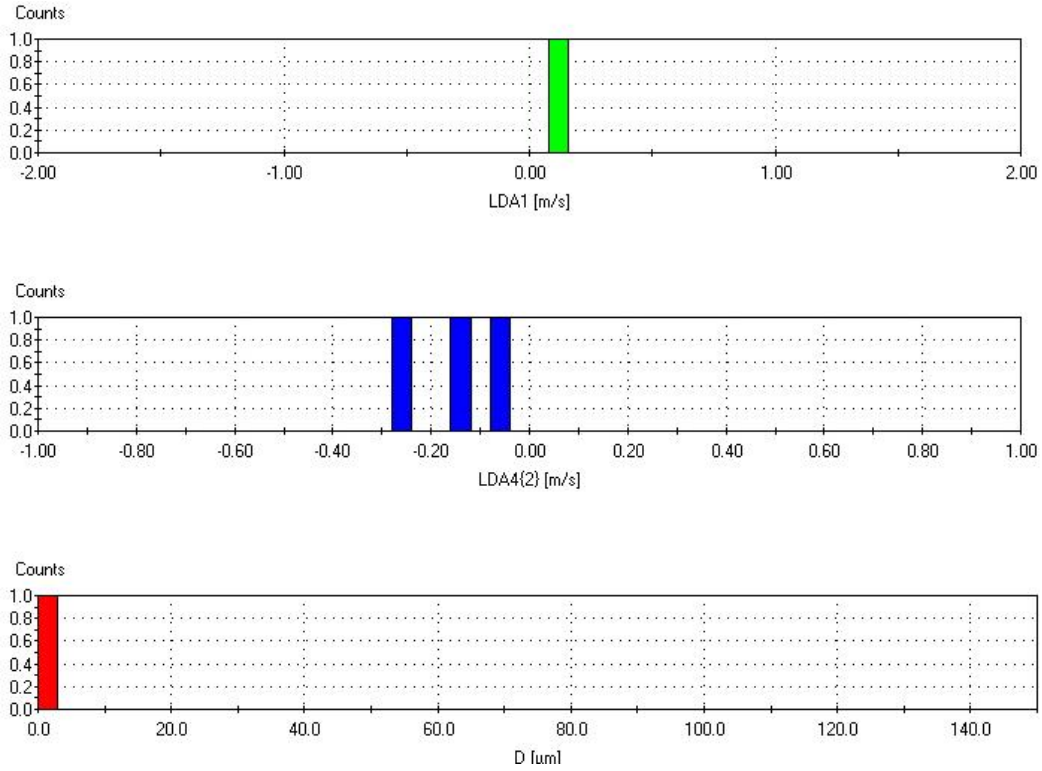

Figure 4.35: BSA Flow Software data sheet example

CHAPTER 5

RESULTS AND DISCUSSION

In Chapter 5, data collected from BSA Flow Software is tabulated and functioned as project results. Data is analyzed for 5 water flow rates to characterize the bubble flow and behaviour in water flow. An upward force was exerted on both the water and bubbles by water pump and air pump respectively along with gravitational force acting downward of the pipe. Air was injected through a quick release connector at a velocity of 1.5 m/s. In this chapter, discussion is included along with the graphs plotted to show the relationship between sauter mean diameter, horizontal and vertical velocity with the data positions. The results are then compared with the pictures taken during the experiments.

Experiments were repeated for all the data points at a range of motor speed and water flow rate. Unit conversion for motor speed and water flow rate is illustrated in Table 5.1. The maximum motor speed was 1725 rpm. Experiments were carried out for five different water flow rates, 5 gpm, 10gpm, 15 gpm and 20 gpm. The cross sectional area of pipe was calculated using the formula:

$$A = \pi D_i^2/4 \tag{5.1}$$

D_i is the inner diameter of pipe, which is 26 mm (0.026 m), and A is equal to 0.00053 m^2. The velocity of water flowing upward of each water flow rate was calculated by using the equation:

$$V = Q/A \tag{5.2}$$

Q is the water flow rate in m^3/s and V is the water velocity in m/s.

Table 5.1: Unit conversion for motor speed and water flow rate

Water flow rate (gpm)	Water flow rate (m^3/s)	Water velocity (m/s)
5	0.000315	0.5943
10	0.00063	1.1887
15	0.000945	1.7830
20	0.00126	2.3774

5.1 Five gpm Water Flow Rate

5.1.1 Velocity Profile

The horizontal velocity profile of the bubbles in pipe is shown in Figure 5.1 while the vertical velocity profile is shown in Figure 5.2.

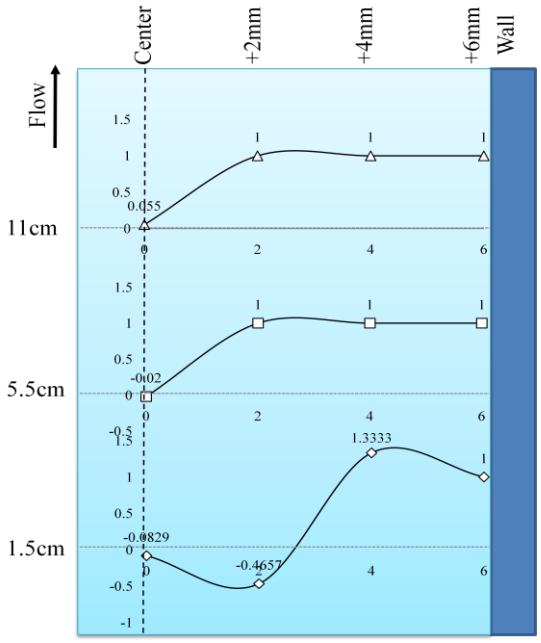

Figure 5.1: Horizontal velocity profile (5 gpm)

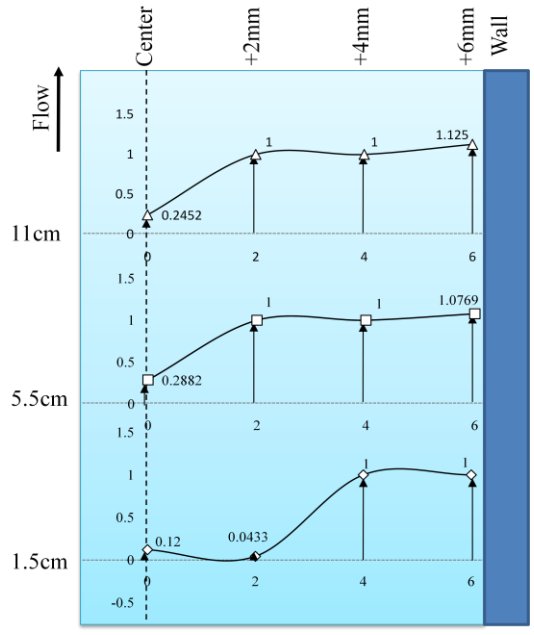

Figure 5.2: Vertical velocity profile (5 gpm)

As the bubbles moved upward, the horizontal velocity at the center of pipe remained constant and even negligible as it was near 0 m/s. The bubbles were rather steady at this region as they only moved in the upward vertical direction. Therefore, the fluid flow at the center of pipe was linear and upward. For 5 gpm of water flow rate, the water velocity was 0.5943 m/s and the bubbles were injected at 1.5 m/s. As the bubbles entered the boundary layer region, their velocity at the center of pipe was smaller than both the water and initial velocity. This could be explained as the mass of air bubble is small, it has less energy and water tends to push the weak mass aside towards the low velocity region, which is the pipe wall. This caused the bubbles to be trapped at the wall. These bubbles merged and became bigger in diameter. This could be the reason that the velocity is higher at the wall than at the center of pipe.

The vertical velocity increased constantly as the bubbles travelled towards the pipe wall could also be explained by using the theory of buoyancy. Buoyancy acted along this path, along with the gravitational downward acceleration, bringing the bubbles upward. The net upward buoyancy force is equal to the magnitude of the weight of fluid displaced by the air bubbles. This force enables the bubbles to float. From the development of velocity boundary layer, due to no-slip condition, the fluid particles in the layer in contact with the surface of the pipe come to a complete stop. As the weight of air (bubbles) is lighter than the weight of water, the density of air is less than water. Thus, the buoyancy of air is greater than its own weight and will float to a level where it displaces the same weight of water as the weight of itself.

Generally, the bubble vertical velocity increased as it moved from elevation 1.5 cm to 5.5 cm. This is parallel with the theory of velocity boundary layer in a pipe for laminar flow whereby the velocity of fluid increases at the center of pipe. After that, the velocity decreased as it entered the 11 cm elevation region whereby the fluid lost its energy as it travelled upward and forces like drag and friction decreased the velocity of fluid.

There was a drastic change in the bubble's horizontal and vertical velocities at an elevation of 1.5 cm above the pipe coupling, 2 mm away from the center of pipe. The horizontal velocity increased while the vertical velocity decreased. This rapid variation of velocity could be a sign of turbulent flow as the particles exhibit additional transverse

motion. The change of direction of the velocities shows the characteristic of eddies. It could be assumed that the fluid swirls and creates reverse current. At the center of pipe where it was nearest to the bubble injection point, the force exerted by the air pump on the bubbles was concentrated. As the bubbles moved away towards the pipe wall, the force was distributed and the horizontal and vertical velocities were almost equal to 1 m/s. This proved that the bubbles were apparently swirling or moving in circular motion.

5.1.1 Sauter Mean Diameter Analysis

Figure 5.3 illustrates the bubbles' sizes in which 1 cm represents a true size of 200 μm. Figure 5.4 is plotted for sauter mean diameter, D_{32} (μm) versus horizontal displacement from the center of pipe (cm) at different elevations above the coupling.

From the graph, it is obvious that the bubbles flowing upward along the center of pipe have a constant size range at different heights of the pipe. This indicates that the flow at the center of pipe was a bubble flow, where the air pumped into the pipe moved as small dispersed bubbles through a continuous fluid. Also, it is true that bubble flow occurs at low flow rate and low holdup of the bubbly fluid. In bubbly flow, each fluid moves at a different speed due to different gravitational forces and other factors, like wall drag and upward forces, with the heavier phase (water) moving slower, or being held up, than the lighter phase (bubbles/air).

At 2 mm away horizontal from the center of pipe, the bubbles showed a significant small size of diameter. A possible explanation would be those bubbles with extremely small diameter could be small droplets of water trapped in large bubbles, whereby only the small droplets were detected by the receiving probe. This could be a phenomenon caused by slug flow where the water and gas velocity is relatively low and slug refers to heavier and slower moving fluid.

As the bubbles moved towards the pipe wall, the diameter increased dynamically, especially at higher elevation. This is due to the effect of buoyancy force. From the development of velocity boundary layer, due to no-slip condition, the fluid particles in the layer in contact with the surface of the pipe come to a complete stop. As the weight of

air (bubbles) is lighter than the weight of water, the density of air is less than water. Thus, the buoyancy of air is greater than its own weight and will float to a level where it displaces the same weight of water as the weight of itself. In the mean time, as the bubbles slowed down at the wall, they merged or agglomerated and become bigger. Those bubbles at the centerline, which are faster, have less chance to merge.

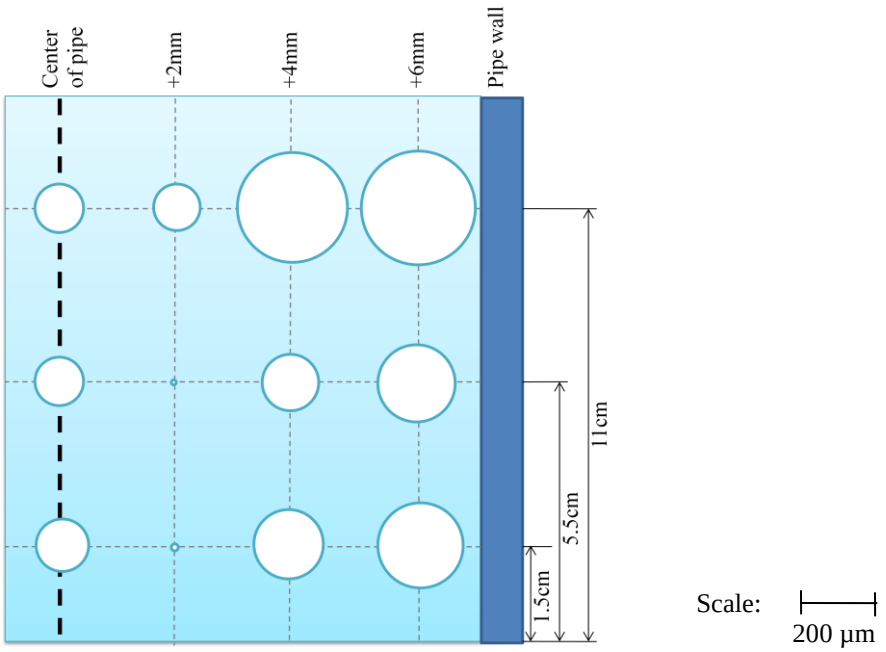

Figure 5.3: Bubble diameter illustration (5 gpm)

(a) Vertical displacement = 11 cm

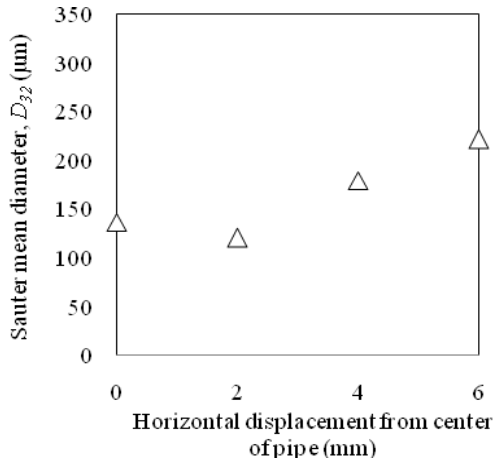

(b) Vertical displacement = 5.5 cm

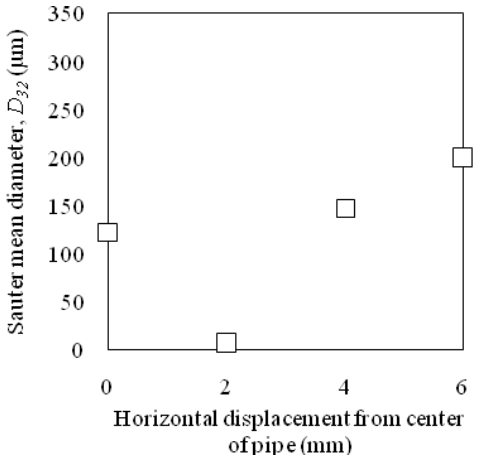

(c) Vertical displacement = 1.5 cm

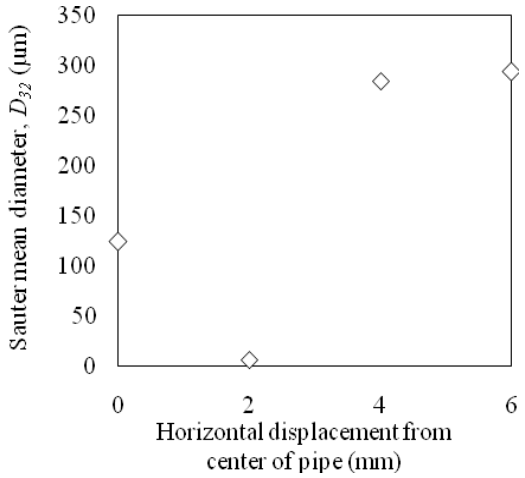

Figure 5.4: D_{32} versus horizontal displacement from center of pipe

5.2 Ten gpm Water Flow Rate

5.2.1 Velocity Profile

The horizontal velocity profile of the bubbles in pipe is illustrated in Figure 5.5 while the vertical velocity profile is illustrated in Figure 5.6.

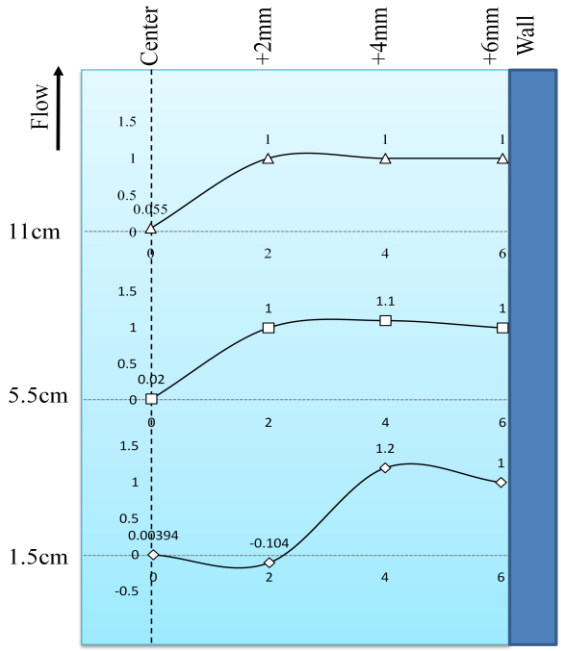

Figure 5.5: Horizontal velocity profile (10 gpm)

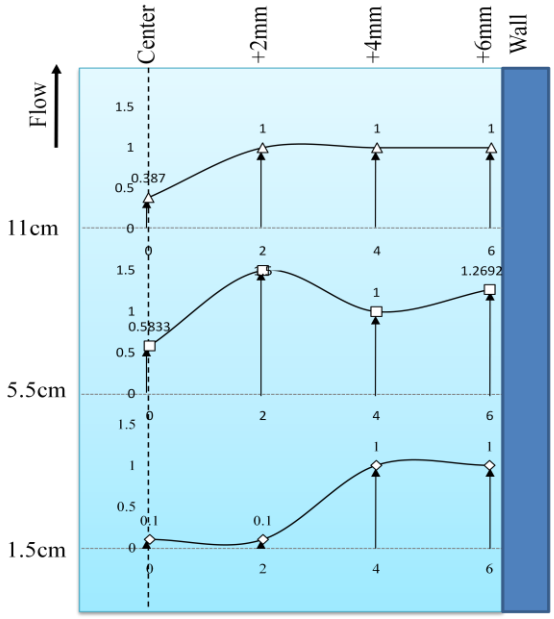

Figure 5.6: Vertical velocity profile (10 gpm)

At water flow rate of 10 gpm, the horizontal velocity at the center of pipe remains constant, which was near 0 m/s, as the bubbles moved upward. However, vertical velocity at this path increased as the bubbles moved downstream. With near 0 m/s value of horizontal velocity, this flow is defined as laminar flow, in which there is no disruption of motion. This might be due to the position of the flow path, which is at a distance away from the pipe wall. Thus, it is not affected by the wall drag. The bubbles were rather steady at this region as they only moved in the upward vertical direction. Therefore, the fluid flow at the center of pipe was linear and upward.

The water velocity was 1.1887 m/s and the bubbles were injected at 1.5 m/s. As the bubbles entered the boundary layer region, their velocity at the center of pipe was smaller than both the water and initial bubbles' velocity. This could be explained that the mass of air bubble is small, it has less energy and water, which has larger mass, tends to push the weak mass aside towards the low velocity region, which is the pipe wall. This caused the bubbles to be trapped at the wall. These bubbles agglomerated and became bigger in diameter. This could be the reason that the velocity is higher at the wall than at the center of pipe.

Horizontal velocity increased simultaneously with vertical velocity and remained constant as the bubble reached the pipe wall. The rapid variation of velocity shows the characteristic of turbulence as the bubble moves in two directions with relatively similar value of velocity. Assumption could be made that there is formation of eddies as the fluid swirls and moves in circular motion, creating reverse current.

The velocities of bubbles, both horizontal and vertical, at the elevation of 1.5 cm and 5.5 cm above the coupling were higher. This is due to the higher water flow rate as compared to the previous water flow rate. However, the velocities reduce to 1 m/s as the bubbles travels upward until the elevation of 11 cm. In between, there could be a loss of energy, i.e. potential and kinetic energy, caused by drags and friction. Eddies contribute to the viscous dissipation of energy by an inertial and essentially inviscid mechanism. Loss of energy indicates the decrease of fluid velocity.

5.2.1 Sauter Mean Diameter Analysis

Figure 5.7 gives a clearer picture of bubble diameter illustration. The scale of bubble diameter is 1 cm: 200 µm. Figure 5.8 is plotted for sauter mean diameter, D_{32} (µm) versus horizontal displacement from the center of pipe (mm) at different elevation above the coupling.

From the graphs, the bubbles flowing upward at the center of pipe had constant size range at different heights. This is a sign of bubble flow, where the air pumped into the pipe moves as small dispersed bubbles through a continuous fluid. Also, it is true that this bubble flow occurs at a relatively low flow rate (10 gpm) and low holdup of the bubbly fluid. In bubbly flow, each fluid moves at a different speed due to different gravitational forces and other factors, like wall drag and upward forces, with the heavier phase (water) moving slower than the lighter phase (bubbles/air).

At 2 mm away from the center of pipe, all the bubbles showed significantly extreme small sizes of diameter. These bubbles could be the small droplets of water trapped in large bubbles or continuous gas phase, whereby only the small droplets could be detected by the receiving probe. This could be defined as slug flow it occurs at rather low fluid velocity. A proper explanation of slug flow would be a multiphase-flow regime in which most of the lighter fluid (bubbles/air) is contained in large bubbles dispersed within, and pushing along the heavier fluid (water). For slug flow, most of the bubbles coalesced to form the large bubbles until they span much of the pipe. Nevertheless, there are also small bubbles within the liquid.

As the bubbles moved towards the pipe wall, the diameters of bubbles were not stable. The trend is rather indistinct as there is different size ranges, from the smallest to the largest. This could be due to the higher water flow rate (higher than 5 gpm). The air could have moved as large bubbles dispersed within continuous water flow and these large bubbles probably formed by small bubbles coalescence. With the analysis, this flow could possibly be plug flow or slug flow because it contains both small and large bubbles. This phenomenon could also happen due to the decrease of velocity due to drag and friction. This contributes to the forming of plug and slug flow. Drag could be caused by pipe wall or the fluid itself. Drag or fluid resistance is the forces that oppose the relative

motion of an objective through fluid. In this case, the drag forces act downward, which is the opposite direction of the oncoming flow velocity. Unlike drag which is dependent on the velocity of fluid, friction is the resisting force between the fluids in contact. In the mean time, as the bubbles slowed down at the wall, they merged or agglomerated and became bigger. Based on the development of boundary layer, those bubbles at the centerline, which are faster, have less chance to merge.

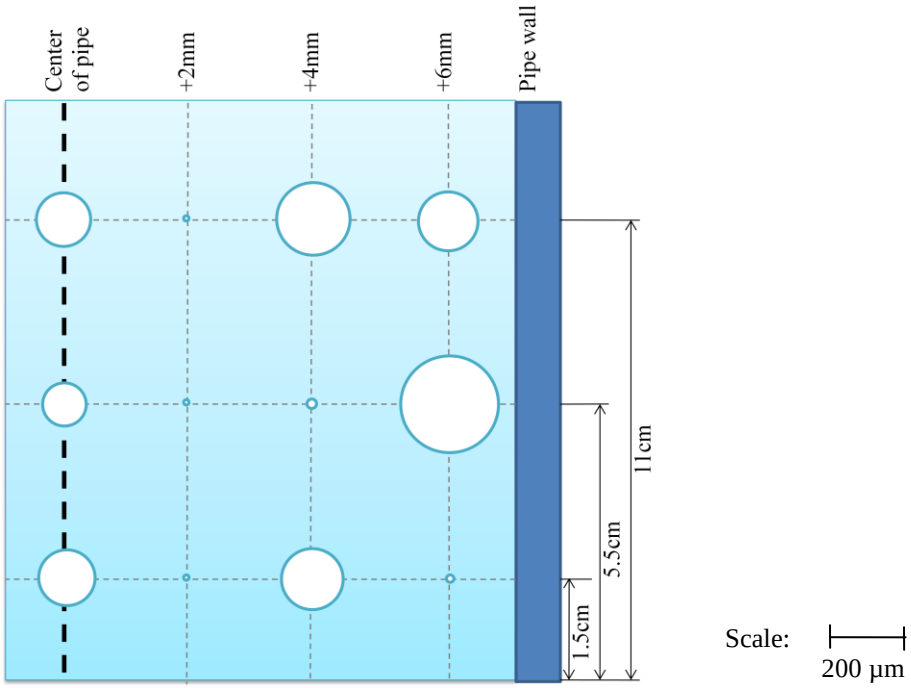

Figure 5.7: Bubble diameter illustration (10 gpm)

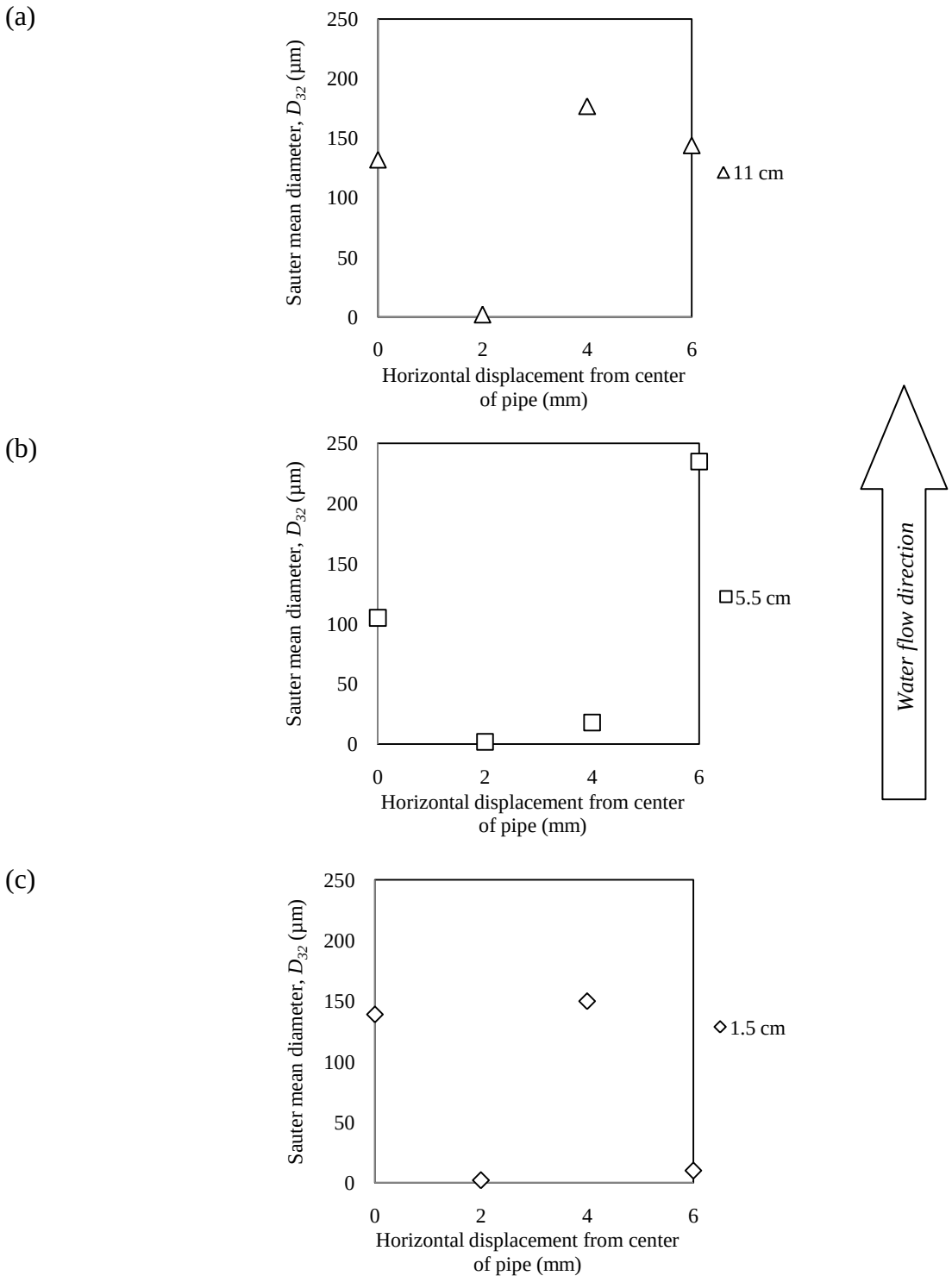

Figure 5.8: D_{32} versus horizontal displacement from center of pipe

5.3 Fifteen gpm Water Flow Rate

5.3.2 Velocity Profile

The horizontal velocity profile of the bubbles in pipe is illustrated in Figure 5.9 while the vertical velocity profile is illustrated in Figure 5.10.

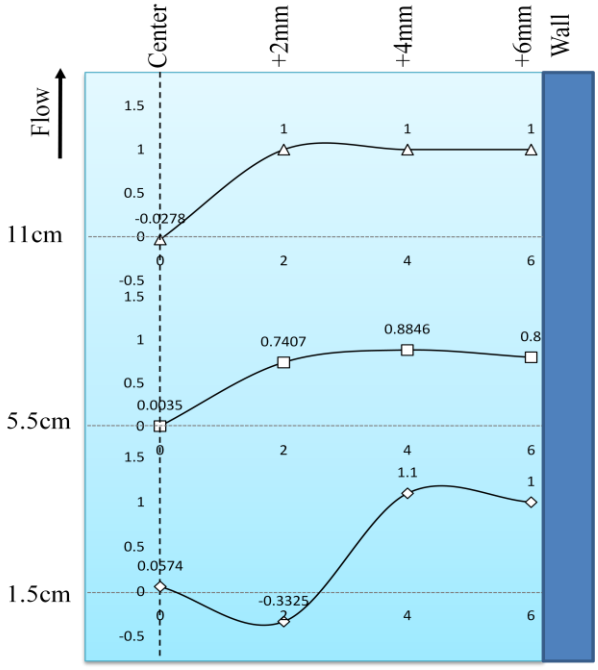

Figure 5.9: Horizontal velocity profile (15 gpm)

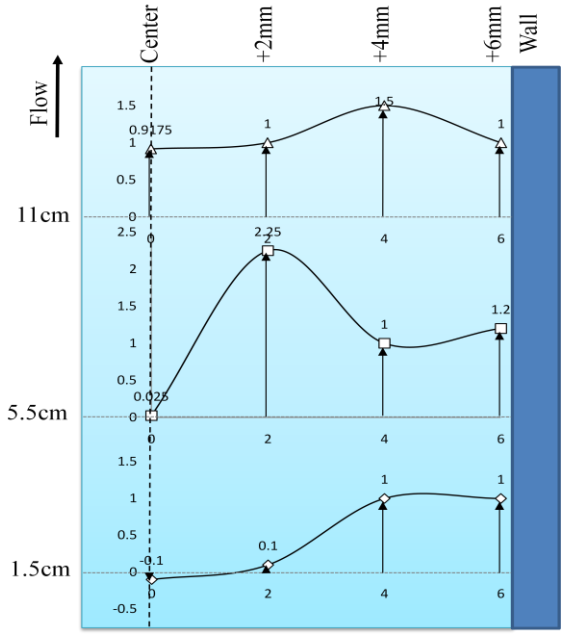

Figure 5.10: Vertical velocity profile (15 gpm)

At 15 gpm of water flow rate, the horizontal velocity at the center of pipe remained constant, which was close to 0 m/s, as the bubbles moved upward. There is a change in direction for horizontal velocity at 1.5 cm elevation. The horizontal velocity at the elevation of 5.5 cm shows smaller value compared to the other heights. Overall, the horizontal velocity increased as the bubble travelled towards the pipe wall. The vertical velocity increased unsteadily as the bubble moved towards the pipe wall. This shows the characteristic of turbulence as the bubble moves in two directions. There is formation of eddies as the fluid swirls and moves in circular motion, creating reverse current.

The water velocity was 1.783 m/s and the bubbles were injected at 1.5 m/s. Bubbles' velocity is lower than water velocity. As the bubbles entered the boundary layer region, their velocity at the center of pipe was smaller than both the water and initial bubbles' velocity. This could be explained that the mass of air bubble is small, it has less energy and water, which has larger mass, tends to push the weak mass aside towards the low velocity region, which is the pipe wall. This caused the bubbles to be trapped at the wall. These bubbles agglomerated and became bigger in diameter. This could be the reason that the velocity is higher at the wall than at the center of pipe.

A concrete evidence of turbulence is the drastic change in the bubble's horizontal velocity at an elevation of 1.5 cm above the pipe coupling, 2 mm away from the center of pipe. The change of direction of the velocities shows the characteristic of an eddy. It could be assumed that the fluid swirls and creates reverse current.

The fluid is flowing at a high velocity. Based on the theory of velocity boundary layer, the velocity at the center of pipe will increase as the velocity profile is fully developed and the friction exerted by pipe wall makes the fluid comes to a complete stop. Thus the vertical velocity increased around the center of pipe.

As the bubbles travelled towards the pipe wall, the vertical velocity decreased and became constant. Buoyancy acts along this path, along with the gravitational downward acceleration, forcing the bubbles to move upward. The net upward buoyancy force is equal to the magnitude of the weight of fluid displaced by the air bubbles. This force enables the bubbles to float. As the weight of the bubbles is lighter than the weight of

water, the density of bubbles is less than water. Thus, the buoyancy of air is greater than its own weight and will float to a level where it displaces the same weight of water as the weight of itself. Due to the reducing pressure at an increasing elevation, the bubble rises at an increasing vertical velocity.

5.3.1 Sauter Mean Diameter Analysis

Figure 5.11 gives a clearer picture of bubble diameter illustration. The scale of bubble diameter is 1 cm: 200 μm. On the other hand, Figure 5.12 is plotted for sauter mean diameter, D_{32} (μm) versus horizontal displacement from the center of pipe (cm) at different elevation above the coupling.

By comparing the three graphs, it is obvious that the bubbles flowing upward at the center of pipe, 2 mm and 4 mm away from center of pipe showed a significant change in multiphase flow regime. The flow regime is identified as churn or froth flow whereby large, irregular slugs of air move up the center of pipe, usually carrying droplets of water with them. The remaining water flows up along the pipe walls. The phases are not continuous. The air slugs are relatively unstable, and take on large, elongated shapes. At a water flow rate of 15 gpm, it could be concluded that churn or froth flow occurs at high velocity.

As the remaining water will flow up along the pipe walls, the theory of boundary layer applies. Due to no-slip condition, the fluid particles in the layer in contact with the surface of the pipe come to a complete stop. As the bubbles move towards the pipe wall, the diameter increases dynamically, especially at higher elevation. This is due to the effect of buoyancy force. As the weight of air (bubbles) is lighter than the weight of water, the density of air is less than water. Thus, the buoyancy of air is greater than its own weight and will float to a level where it displaces the same weight of water as the weight of itself. At the mean time, the fact that air is compressible explains the increment in bubble diameter further downstream. As the mass of air bubble is small, it has less energy and water, which has larger mass, tends to push the weak mass aside towards the low velocity region, which is the pipe wall. This caused the bubbles to be trapped at the wall. These bubbles agglomerated and became bigger in diameter. Those bubbles at the centerline, which are faster, have less chance to merge.

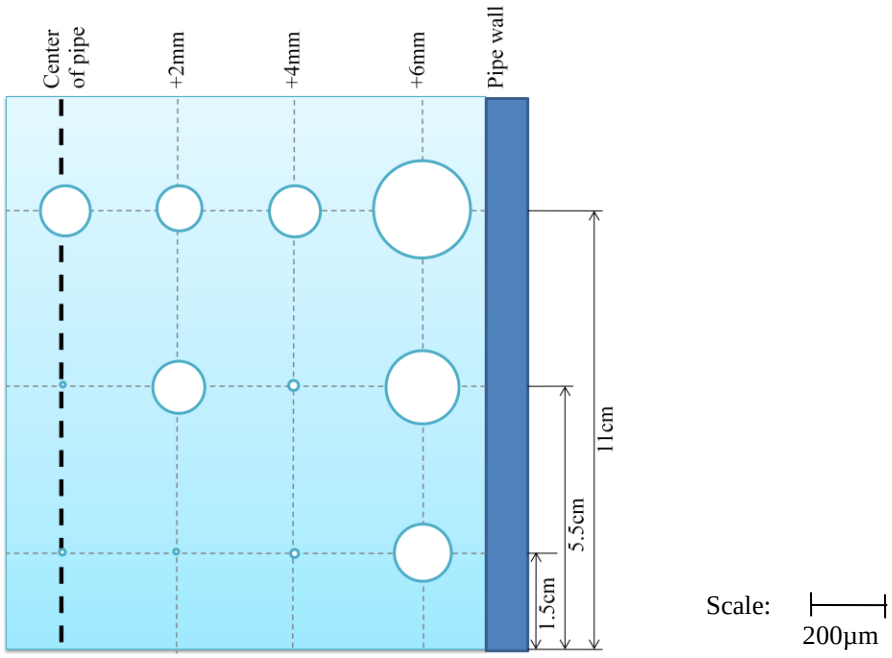

Figure 5.11: Bubble diameter illustration (15 gpm)

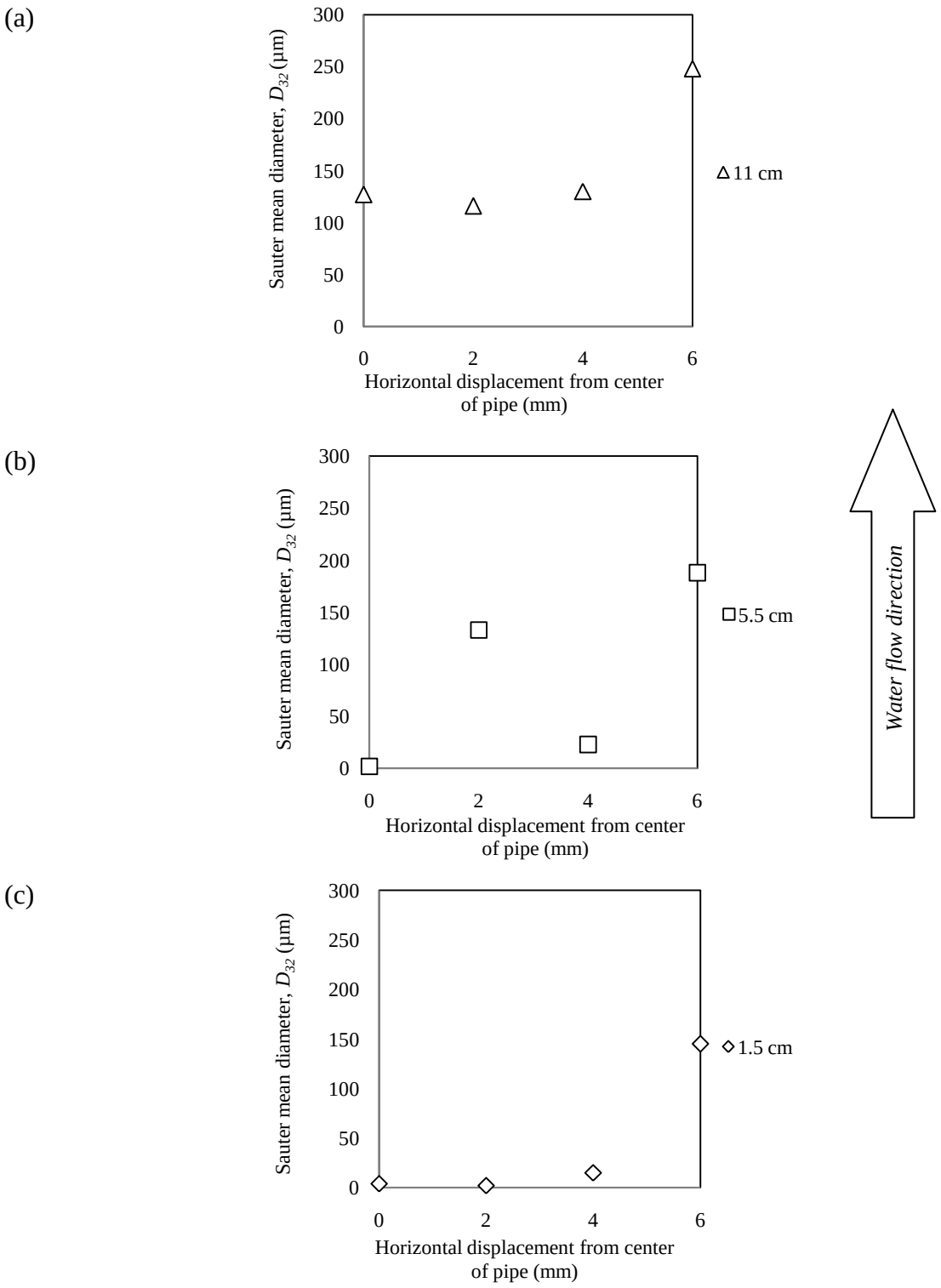

Figure 5.12: D_{32} versus horizontal displacement from center of pipe

5.4 Twenty gpm Water Flow Rate

5.4.2 Velocity Profile

The horizontal velocity profile of the bubbles in pipe is illustrated in Figure 5.13 while the vertical velocity profile is illustrated in Figure 5.14.

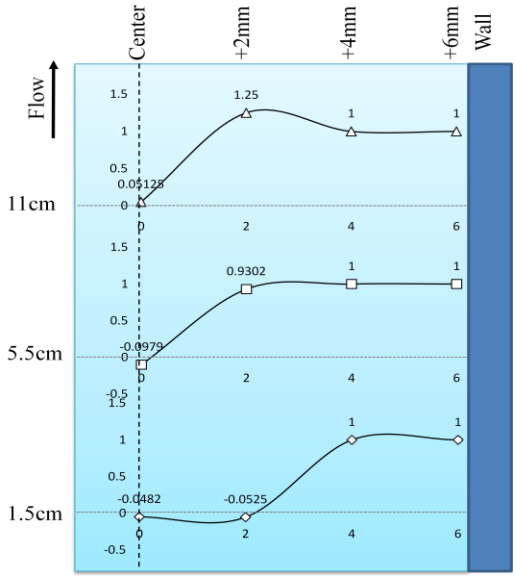

Figure 5.13: Horizontal velocity profile (20 gpm)

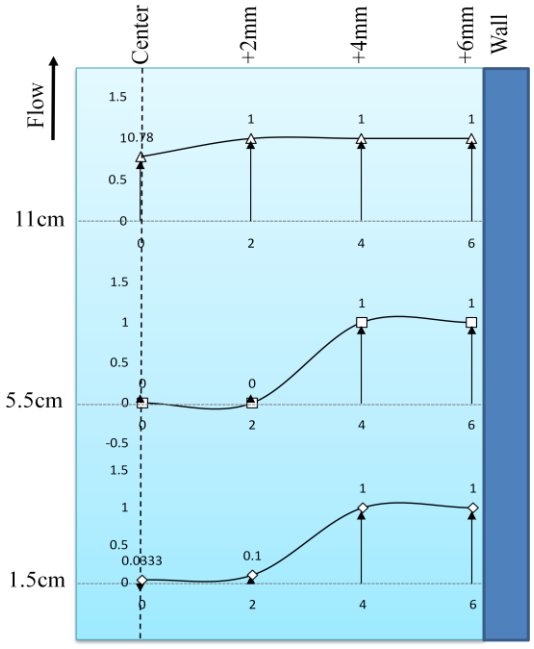

Figure 5.14: Vertical velocity profile (20 gpm)

At 20 gpm of water flow rate, the horizontal velocity at the center of pipe remained constant, which was close to 0 m/s, as the bubbles moved upward. The value of horizontal velocity, regardless of positive or negative value, increased at 2 mm away from the center of pipe. The horizontal velocity at 4 mm and 6 mm away from the center of pipe remained constant.

The water velocity was 2.3774 m/s and the bubbles were injected at 1.5 m/s. Bubbles' velocity was lower than water velocity. As the bubbles entered the boundary layer region, their velocity at the center of pipe was smaller than both the water and initial bubbles' velocity. This is because the mass of air bubble is small, it has less energy and water, which has larger mass, tends to push the weak mass aside towards the low velocity region, which is the pipe wall. This caused the bubbles to be trapped at the wall. These bubbles agglomerated and became bigger in diameter. This could be the reason that the velocity is higher at the wall than at the center of pipe.

Bubble vertical velocity was rather constant as the bubbles moved upward along the center of pipe until it reached 11 cm of height. At 1.5 cm and 5.5 cm of height, the vertical velocity increased slowly and remained constant when it approached the pipe wall. At 11 cm of height the vertical velocity was rather constant from the center to the wall of pipe.

By comparing the velocity profiles, it is obvious that the range of velocity for both horizontal and vertical is almost equivalent. Thus, the bubbly flow could be determined as turbulent flow. Bubbles are swirling and moving in circular path and this phenomenon is called eddies.

5.4.1 Sauter Mean Diameter Analysis

Figure 5.15 and Figure 5.16 shows the bubble diameter trend at 20 gpm of water flow rate.

At 20 gpm of water flow rate, the bubble sizes range is extreme. Most of the bubbles were of very small sizes while the other half were of significantly large sizes. There was a constant increase in bubble size at 11 cm of height. This shows the multiphase flow regime called mist flow, in which water exists as very small, approximately homogeneously distributed droplets. Mist flow occurs at high velocities.

At 11 cm elevation, as the bubbles travelled towards the pipe wall, the diameter of bubbles increased. When the bubbles reached that elevation, due to the reducing pressure, the bubble rose at an increasing vertical velocity. It could be observed that the bubble near pipe wall is the largest. This could be due to the smaller mass that air bubbles have than water. As bubbles are of less energy, water tends to push the weak mass aside towards the low velocity region, which is the pipe wall. This caused the bubbles to be trapped at the wall. These bubbles agglomerated and became bigger in diameter. Those bubbles at the centerline, which are faster, have less chance to merge.

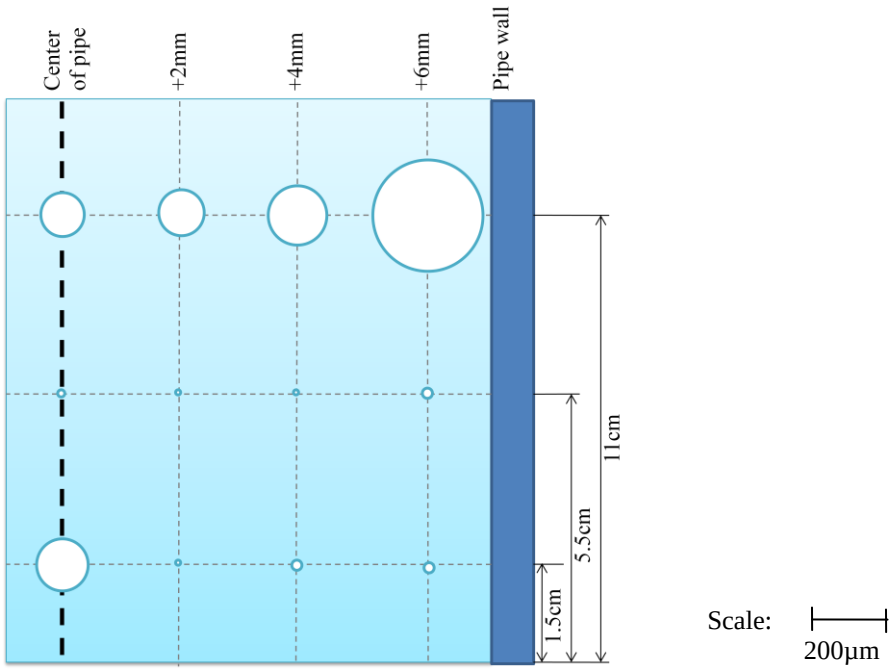

Figure 5.15: Bubble diameter illustration (20 gpm)

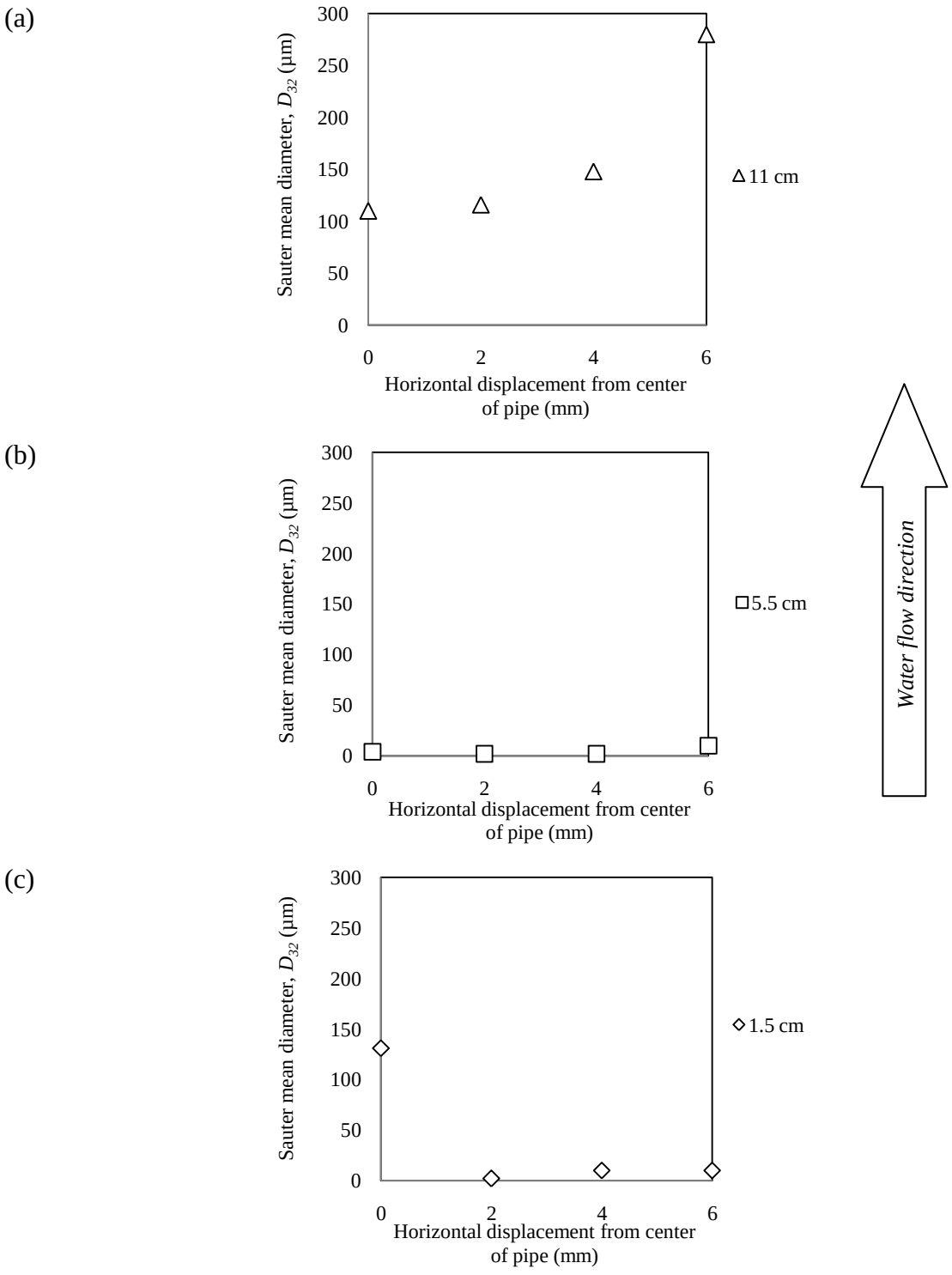

Figure 5.16: D_{32} versus horizontal displacement from center of pipe

5.5 Bubbles Image

(a) 5 gpm

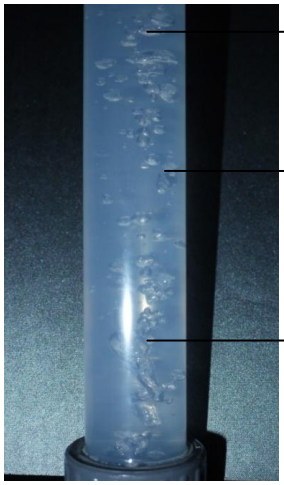

(b) 10 gpm

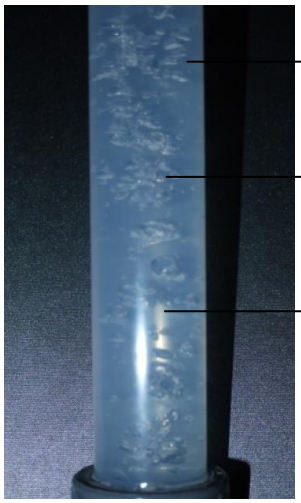

(d) 15 gpm

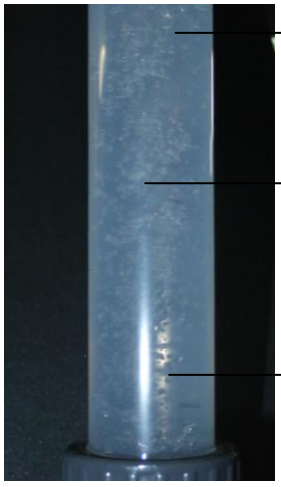

(e) 20 gpm

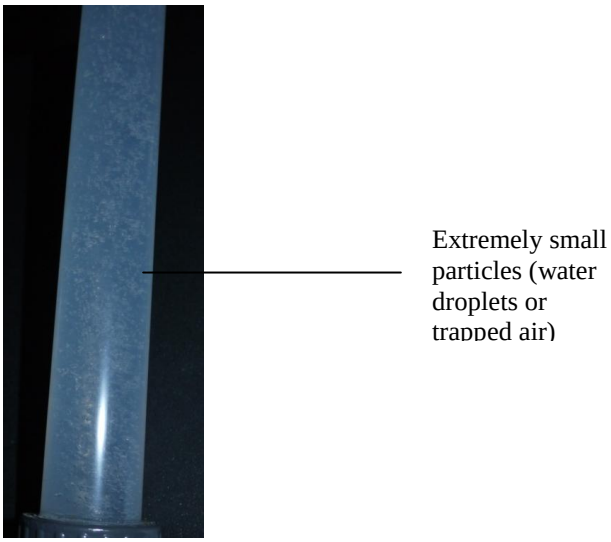

Figure 5.17: Picture of bubbles at different water flow rates

Figure 5.17 gives a real illustration of bubbles in pipe at different water flow rates. The pictures shows the same results from the data collected. At higher elevations, the bubble sizes are relatively larger while at lower elevations the sizes are smaller. At near pipe wall area, the bubble sizes also increases due to the coalescence of bubbles to form larger bubbles. Sign of turbulence or swirling could be detected at the center of pipe. Constant bubble diameter is determined to happen at the center of pipe. At lower water flow rates, the bubbles are lesser and have larger diameters. At higher water flow rates, the bubbles are of very small diameters and great in amount. Extremely small bubble sizes are not significant in these pictures but it could be explained by small particles of water droplets or trapped air in larger bubbles. The receiving probe could only detect the small particles trapped and thus displayed extremely small sizes.

5.6 Effect of Boundary Layer on Distribution of Bubbles

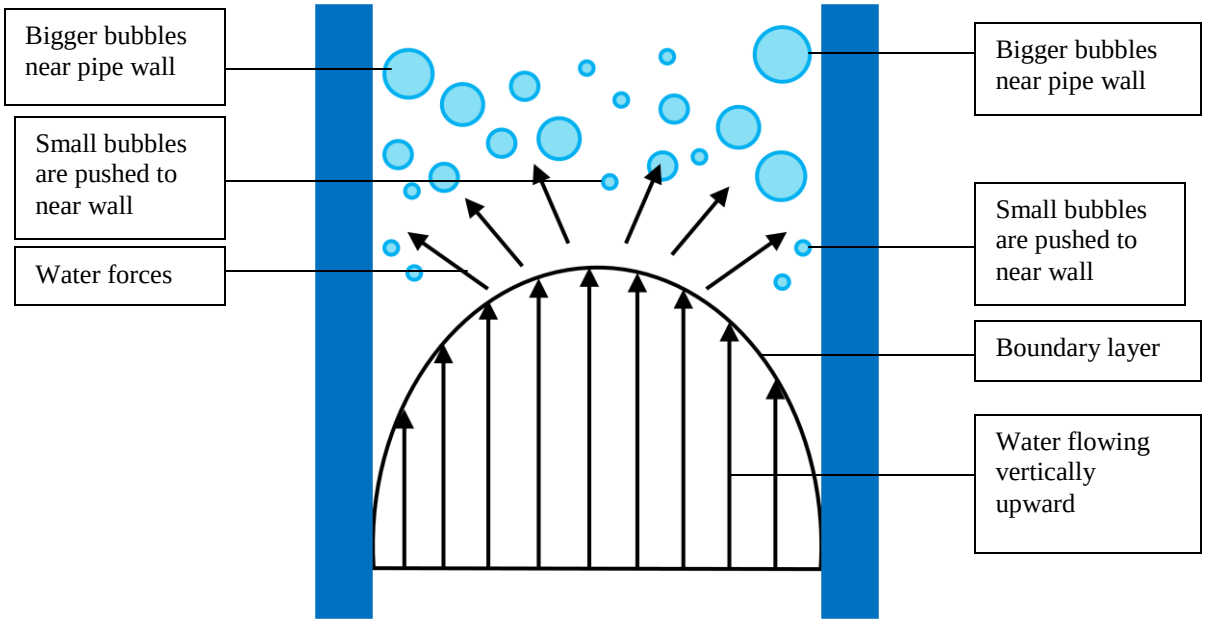

Figure 5.18: Effect of boundary layer on distribution of bubbles

Figure 5.18 shows the effect of laminar boundary layer on the distribution of bubbles. The velocity of bubbles is lesser than the velocity of water. The mass of air bubbles is small, thus it has less energy. Water, which is of greater mass and higher energy level, pushes the weak mass of air aside towards the low velocity region. This low velocity region refers to the pipe wall. At the pipe wall region, these bubbles slow down, merge and become bigger in size. At the centerline of the boundary layer, the water flow is faster and bubbles have less chance to merge.

CHAPTER 6

CONCLUSIONS AND RECOMMENDATIONS

5.1 Conclusions

In conclusion, the existence of bubbles in liquid flow creates multiphase fluid flow. The bubbles in liquid flow changes its characteristics when it travels from center of pipe to near pipe wall and from lower elevation to higher elevation. Water flow rate is another

factor that affects the behavior of the bubbles. The changes could be determined by detecting the diameters, horizontal and vertical velocity of bubbles at different data points. The experiment results collected from the lab are tabulated into useful data for further investigation. Different multiphase flow regimes could be recognized from the trend displayed by diameters and velocities. These flow regimes, for example slug, froth and annular flow, show that the fluid flow is affected by boundary layer, buoyancy force, drags and frictions.

The results from the experiments show variations in bubble diameter, from very large bubbles, which is up to near 300 μm, to extremely small bubbles, which is around 2 μm. Very large bubbles normally occur near pipe wall at where the heavier medium, which is water, would travel slower. Based on the development of velocity boundary layer, water is flowing at minimum velocity near pipe wall and maximum velocity at the center of pipe. Therefore, the bubbles that travel along the near pipe wall path are subjected to high buoyancy force. As the bubbles travel downstream to a higher elevation, the decrease of pressure results in the increase of bubble volume.

At the center of pipe, the bubble diameters are quite constant and display a size range of 100-140 μm for lower water flow rates i.e. 5 gpm, 10 gpm, and 10.5 gpm. The absence of pipe wall drag at the center of pipe and minimum flow rate at pipe wall make water flowing at higher velocity at the center path. Thus, buoyancy force does not take place. Along the path of 2 mm away from center of pipe, the fluid flow normally display extremely small bubbles at lower elevation. This could be due to small particles, either water droplets or trapped air, in larger air bubbles. This phenomenon is called slug flow for low velocity medium and annular flow for high velocity medium.

The horizontal velocity at the center of pipe for all water flow rates is near 0 m/s and indicates that the fluid flow is laminar. As the bubbles move towards pipe wall, the fluid flow becomes turbulent. The horizontal and vertical velocities increase and have nearly same value, which is around 1 m/s. An assumption could be made that the bubbles swirl and move in circular motion in which it could be defined as eddies.

From the experiments conducted and results obtained, the project is successful and the objectives to study the characteristics of bubbles in water flow are achieved.

5.2 Recommendations

For recommendations, the experiment should be carried out on different pipe orientations, for example using inclination, horizontal and vertical downward pipes. The experiment results could be compared to the results obtained in this project. However, efforts are needed in the designs of the pipe system and new parts should be purchased to suit the position of pipe. Other than that, the characteristics of bubbles in water flow could be examined at different parts of the pipe system, for example elbow and junctions. The pipe system could also be modified the shape and the diameter of the pipe. The length of the pipeline could be one of the variables and from there the effect of pressure drop could be investigated. More data points should be added from pipe wall to pipe wall. This way, the diameter and velocity trends would be more significant.

The fluids could be of more varieties. Water could be replaced by other liquids with different properties like oil, distilled water, or other chemicals which would relate to the real industries nowadays. These liquids could have different weight, density, chemical properties and viscosity. The effect of buoyancy could be examined. Contaminants like sands and mud could be added to the fluid flow to enlarge the area of investigation. As for the bubbles, atmospheric air could be replaced by other types of gases, as for example, nitrogen, carbon dioxide, and natural gas. They could also differ in terms of the concentrations.

Other effects of bubbles could be examined by modifying this project. The effect of vibration as a factor of the presence of vibrant bubbles in pipeline could be one of the options to improve this project. Vibration could be induced by changing the oscillation amplitude of dynamic bubbles. With increasing frequency and unstable fluid flow in pipe, vibration could be observed. In addition, experiment could be performed on a bubble subject to vertical vibration. With the presence of vibration, the physical characteristics of bubbles could be observed.

As the trend of bubble velocity is quite constant, a prediction of velocity profile is made for water flow rate of 5 gpm. Figure 6.1 and Figure 6.2 are predictions of bubble horizontal and vertical velocities of further upstream made by analyzing the trend of the velocity displayed at higher elevation.

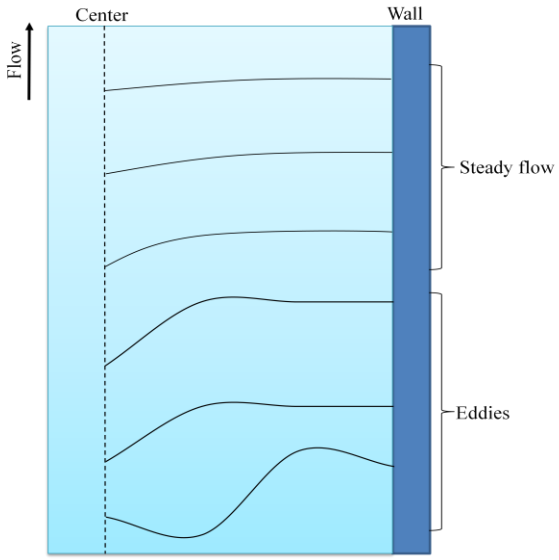

Figure 6.1: Horizontal velocity prediction

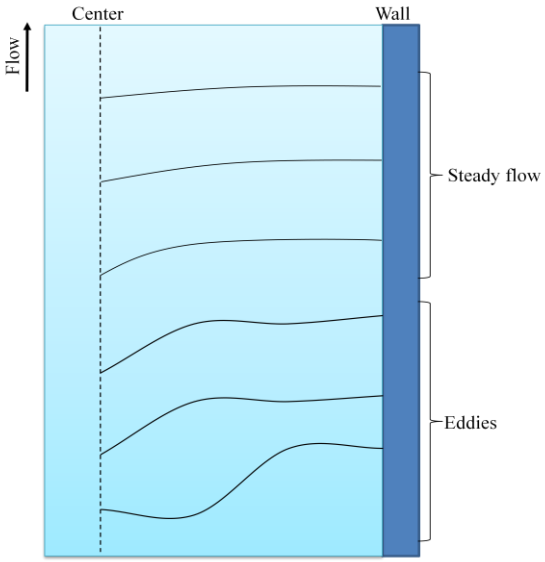

Figure 6.2: Vertical velocity prediction

References

Andrews, D. B. (2004) Fundamentals of Cavitations and Selection of Pumps, *Lawrence Pumps Inc. Run Times Volume 1 Issue 5*, Massachussets.

Brennen, C. E. (2005) Fundamentals of Multiphase Flow. *Cambridge University Press*, California.

Cengel, Y. A. and Cimbala, J. M. (2006) Fluid Mechanics Fundamentals and Applications. *McGraw-Hill International Edition*, Singapore.

Corradini, M. L. (1997) Multiphase Formulation and Pressure. *CDT*.

Dantec Dynamics (2010) Laser Doppler Anemometry, Particle Dynamics Analysis – Measurement Principles. *Laser Optic Measurement Systems and Sensors*.

Descamps, M. N., Oliemans, R. V. A., Ooms, G. and Muddle, R. F. (2008) Air-water Flow in a Vertical Pipe: Experimental Study of Air Bubbles in the Vicinity of the Wall. *Open Access Research Articles*.

Fomin, N.A. (2009) Analysis of Three-Dimensional Structures in Complex Turbulent Flows. *Journal of Engineering Physics and Thermophysics*, **82**.

Hale, R. (2009) < http://www.ehow.com/about_5095742_weather-vane-measure.html>

Herbert, O., Prandtl, L. (2004) Prandtl's essentials of fluid mechanics Volume 158 of Applied mathematical sciences Prandtl's Essentials of Fluid Mechanic. *Springer*, Germany.

Kundu, P. K. and Cohen, I. M. (2008) Fluid Mechanics. *Academic Press*, London.

Lefebvre, A. H. (1989) Atomization and Sprays. *Hemisphere Publishing*. New York.

Lima-Ochoterana R. and Zenit R. (2003) Visualization of the Flow around a Bubble Moving in a Low viscosity Fluid. *Institude of Material Investigation*, Mexico.

Lindken, R. and Merzkirch, W. (2000) Velocity Measurements of Liquid and Gaseous Phase for a System of Bubbles Rising in Water. *Experiments in Fluids*, S194-S201.

Liu, H. (2003) Piping Engineering: Fundamentals for the Water and Wastewater Main Operator Series. *CRC Press*, Ohio.

Lu, J. and Tryggvason, G. (2007) Effect of Bubble Size in Turbulent Bubbly Downflow in a Vertical Channel. *Chemical Engineering Science*.

Lu, J., Fernandez, A. and Tryggvason, G. (2005) The Effect of Bubbles on the Wall Drag in a Turbulent Channel Flow. *Physics Fluids*, **17**.

Manning, F. S. and Thompson, R. E. (1995) Oilfield Processing of Petroleum: Crude oil Volume 2 of Oilfield Processing of Petroleum. *Penwell Books*, New York.

McCain, W. D. Jr. (1990) The Properties of Petroleum Fluids Second Edition. *PennWell Publishing Company*, Oklahoma.

Murai, Y., Fukuda, H., Oishi, Y., Kodama, Y. and Yamamoto, F. (2007) Skin Friction Reduction by Large Air Bubbles in a Horizontal Channel Flow. *International Journal Multiphase Flow*, **33**, 147-163.

Nakamura, Y., Usuda, S. and Morishita, S. (2007) A Research of Bubbling Generation Technology and Application Using City Water Pressure. *Proceeding of International Conference on Electrical Machines and Systems 2007*, 1887-1888.

Razzaque, M. M., Afacan, A., Liu, S., Nandakumar, K., Masliyah, J. H. and Sanders, R.S. (2003) Bubble Size in Coalescence dominant regime of turbulent air-water flow through horizontal pipes. *International Journal of Multiphase Flow*.

Rawle, A. (2005) Particle Sizing – An Introduction. *Scientific Information on Colloidal Silver*.

Schick, R. J. (1997) An Engineer's Practical Guide to Drop Size. *Spraying Systems Co.*, Bulletin No. 459.

Schlumberger (2009) < www.slb.com/content/services/artificial/**gas**/index.asp>

Shames, I.H. (2003) Mechanics of fluids. *McGraw-Hill series in mechanical engineering,Engineering Series*, Fairfield.

Shawkat, M. E., Ching, C.Y. and Shoukri, M. (2008) Bubble and Liquid Turbulence Characteristics of Bubbly Flow in a Large Diameter Pipe. *International Journal of Multiphase Flow*.

Sleigh, A. (2009) <http://www.efm.leeds.ac.uk/CIVE/CIVE1400/Section4/laminar_turbulent.htm>

Speight, J. G. (2001) Chemical and process design handbook McGraw-Hill handbooks. *McGraw-Hill Professionals*, Fairfield.

Stewart, M. (2008) Surface Production Operations: Design of Oil Handling Systems and Facilities Third Edition, **1**.

van der Geld, C. W. M., van Wingaarden, H. and Brand, B. A. (2001) Experiments on the Effect of Acceleration on the Drag of Tap Water Bubbles. *Experiments in Fluids*, **31**, 710-713.

Xing, Y. and Hadzic, I. (2004) Cavitating Fuel Pump. *Application Briefs from FLUENT*, **EX224**.

APPENDICES

Sauter mean diameter at 5 gpm

D_{32} vs Horizontal Displacement (1.5 cm)

Horizontal Displacement (mm)	D_{32} (µm)
0	125
2	7
4	285
6	294

D_{32} vs Horizontal Displacement (5.5 cm)

Horizontal Displacement (mm)	D_{32} (µm)
0	122
2	6
4	147
6	199

D_{32} vs Horizontal Displacement (11 cm)

Horizontal Displacement (mm)	D_{32} (µm)

0	136
2	120
4	179
6	221

Sauter mean diameter at 10 gpm

D_{32} vs Horizontal Displacement (1.5 cm)

Horizontal Displacement (cm)	D_{32} (µm)
0	139
2	2
4	150
6	10

D_{32} vs Horizontal Displacement (5.5cm)

Horizontal Displacement (cm)	D_{32} (µm)
0	105
2	2
4	18
6	235

D_{32} vs Horizontal Displacement (11 cm)

Horizontal Displacement (cm)	D_{32} (µm)
0	132
2	2
4	177
6	144

Sauter mean diameter at 10.8 gpm

D_{32} vs Horizontal Displacement (1.5 cm)

Horizontal Displacement (cm)	D_{32} (µm)
0	131
2	2
4	154
6	139

D_{32}vs Horizontal Displacement (5.5 cm)

Horizontal Displacement (cm)	D_{32} (µm)
0	133
2	2
4	138
6	194

D_{32}vs Horizontal Displacement (11 cm)

Horizontal Displacement (cm)	D_{32} (µm)
0	120
2	118
4	103
6	278

Sauter mean diameter at 15 gpm

D_{32}vs Horizontal Displacement (1.5 cm)

Horizontal Displacement (cm)	D_{32} (µm)

0	4
2	2
4	15
6	145

D_{32}vs Horizontal Displacement (5.5 cm)

Horizontal Displacement (cm)	D_{32} (µm)
0	2
2	133
4	23
6	188

D_{32}vs Horizontal Displacement (11 cm)

Horizontal Displacement (cm)	D_{32} (µm)
0	127
2	116
4	130
6	248

Sauter mean diameter at 20 gpm

D_{32}vs Horizontal Displacement (1.5 cm)

Horizontal Displacement (cm)	D_{32} (µm)
0	131
2	2
4	10
6	10

D_{32}vs Horizontal Displacement (5.5 cm)

Horizontal Displacement (cm)	D_{32} (µm)
0	4
2	2
4	2
6	10

D_{32}vs Horizontal Displacement (11 cm)

Horizontal Displacement (cm)	D_{32} (µm)
0	110
2	116
4	148
6	280